SEAL STRENGTH MODELS FOR MEDICAL DEVICE TRAYS

A Dissertation

by

PATRICIA MAYS

Submitted to the Office of Graduate Studies of
Texas A&M University
in partial fulfillment of the requirements for the degree of

DOCTOR OF PHILOSOPHY

May 2008

Major Subject: Industrial Engineering

SEAL STRENGTH MODELS FOR MEDICAL DEVICE TRAYS

A Dissertation

by

PATRICIA MAYS

Submitted to the Office of Graduate Studies of
Texas A&M University
in partial fulfillment of the requirements for the degree of

DOCTOR OF PHILOSOPHY

Approved by:

Chair of Committee,	Cesar O. Malave
Committee Members,	Richard M. Feldman
	Donald R. Smith
	Karan L. Watson
Head of Department,	Brett A. Peters

May 2008

Major Subject: Industrial Engineering

ABSTRACT

Seal Strength Models for Medical Device Trays. (May 2008)

Patricia Mays, B.S., University of Arkansas at Fayetteville;

M.S., University of Arkansas at Fayetteville

Chair of Advisory Committee: Dr. Cesar O. Malave

Seven empirical equations were developed for the prediction of seal strength for medical device trays. A new methodology was developed and used for identifying burst and peel locations and comparing burst pressure and peel force. Multiple linear regression was used to fit 76 models, selecting the best models based on the Akaike Information Criterion (AIC) and adjusted R^2 (R^2_{adj}) value of each model. The selected models have R^2_{adj} and prediction R^2 (R^2_{pred}) values of .83 to .94.

Factors investigated for the peel force response were sealing pressure (3 levels), dwell time (3 levels), sealing temperature (3 levels), and adhesive. Additional factors investigated for the burst pressure response were restraining plate gap, and tray volume, height, length-to-width ratio and area. Polyethylene terephthalate-glycol (PETG) trays with Tyvek 1073B lids and two popular water-based adhesives were used. Trays were selected to yield three levels of area and three levels of length-to-width ratio, defining nine package configurations. Packages for burst testing were sealed under a fractional factorial design with 27 treatments. Packages for peel testing were sealed under a 17-point face-centered central composite design. Packages were tested using peel testing following the ASTM F88-07 standard and restrained burst testing with three gap distances following the ASTM F2054-00 standard.

All possible subsets of the factors were evaluated, with the best models selected based on AIC value. Equations were developed to predict peak and average peel force based on sealing process parameters (R^2_{pred} =.94 and .92), burst pressure based on tray and sealing parameters and gap (R^2_{pred} =.94), and four peel force responses based on burst pressure and gap (R^2_{pred} =.83 to .86). Models were validated through cross-validation, using the prediction error sum of squares (PRESS) statistic. The R^2_{pred} was calculated to estimate the predictive ability of each model.

DEDICATION

This dissertation is dedicated

to my children, Vandissa, Ebony, Bryson, and Jordan, who are my inspiration,

to my mother, Gracie, with love and respect,

to my husband, Vincent,

and to all my dear family and friends.

ACKNOWLEDGEMENTS

I first thank Jesus Christ for giving me the aptitude and the strength to complete my course of study and for always providing resources and people in my life to meet all of my needs. To God be the glory.

I would like to thank my committee chair, Dr. Malave, and my committee members, Dr. Feldman, Dr. Smith, Dr. Watson, and Dr. Alberto Garcia-Diaz for their unwavering support and guidance throughout the course of this research. I extend special gratitude to Rich and Alice Feldman and Judy Meeks, whom I can always count on to be standing in my corner, no matter what. I thank Hamdy Taha and Carter Kerk for their words of encouragement that have stayed with me over the years and across the miles.

I owe tremendous thanks to Amcor Flexibles, Boston Scientific Corporation, Perfecseal Corporation, Shimadzu Corporation, and Westpak, Inc. for their generous support.

Finally, I would like to express very special thanks to all of the individuals who expended their energies to provide me with study materials or equipment, assisted with the preparation or testing of samples, or provided other support that was crucial to the completion of the research, including Bob Liesenfelt, Mary Czarnopys, Gilbert Vial, Karen Polkinghorne, Tom Schaffner, Mark Dolan, Tommy To, Nu Ho, Dao Pham, Duc Truong, Renee Zachary, Vincent Mays, Christine Lewis, Ebony Ferrell, Gail Hopkins, Peter Bernabe, Rachel Swaby, Gene Stutz, Bill Martin, David Jenkinson, Walt Ptasienski, Ai Pham, Joe Demers, Jon Phan, Herb Schueneman, Mark Escobedo, Edmund Tang, and Nebojsa Zolotic.

TABLE OF CONTENTS

Page

CHAPTER

LIST OF FIGURES

LIST OF TABLES

TABLE Page

TABLE Page

CHAPTER I

INTRODUCTION

Research summary

The primary research problem addressed in this work was how to develop generally applicable models of seal strength that will have high predictive value. The research approach addressed six aspects of the modeling process that can affect the predictive ability of the resulting model. These aspects are (1)quality of the input data, (2)representativeness of the sample, (3)determination of the candidate model forms, (4)selection of the best model from all candidates, (5)model validation, and (6)assessment of the predictive ability of the model.

This research work developed a new methodology for sample preparation and identification for medical device tray testing, and used this methodology along with sound engineering and statistical principles to evaluate two measures of tensile strength—burst pressure and peel force—and to develop seven new models for the prediction of peel force and burst pressure responses for medical device trays. This research is important because these tools are not currently available, and the lack of these tools contributes to failures of packaging in the field and creates a risk to the safety of medical device recipients.

In the body of this dissertation, three families of models are developed. The first family of models predicts peak peel force and average peel force based on parameters of the sealing process. The second family of models predicts burst pressure based on sealing process parameters and restraining plate gap distance; there is one model in this family. The third family of models predicts peel force responses based on burst pressure and restraining plate gap distance. There are four models in this family, one for each of four response variables: peak force at the burst location, average force at the burst location, lowest peak force within the tray, and lowest average force within the tray. The models that have been developed will contribute to the solution of a very significant problem in the medical device industry.

This dissertation follows the style of *Packaging Technology and Science*.

The dissertation will begin by explaining the background of the problem that is being addressed, then present a review of the relevant literature. The dissertation will continue with the description of a new structured methodology for tray sample preparation and identification, presentation of robust experimental designs for the study of seal strength responses, and presentation of graphical analyses and regression analyses that characterize these responses and produce predictive models for each response.

Background

Patients who are at the receiving end of sterilized medical devices trust in the sterility of those devices. The loss of device sterility can create life-threatening consequences for the patient. Therefore, it is imperative that the sterile medical device package maintain the device in its sterile state during distribution and throughout the period of storage prior to use.

Medical devices that are heavy, bulky, expensive and/or sensitive to handling are typically packaged in rigid trays as opposed to non-rigid pouches. Most rigid medical device packages consist of a thermoformed plastic tray covered by a Tyvek® lid that is coated with an adhesive and heat sealed to the tray. The process of sealing the tray has a critical impact on the ability of the package to provide an effective sterile barrier for the device.

The packaging design process includes the selection of suitable materials and equipment and the determination of the settings for sealing process parameters, with the aim of producing adequate package seal strength. Unfortunately, the effects of these factors have not been quantified in a way that allows prediction of the resulting seal strength at the design phase. Moreover, there are few published seal-strength data that packaging engineers may use for guidance when selecting materials and equipment, developing sealing and testing processes, or validating package designs and sealing processes.

Problem definition

During the package design phase, device manufacturers are required by industry standard to specify the minimum required seal width and seal strength that the package must meet. The seal strength and seal width need to be adequate to maintain closure under the stresses experienced during sterilization,

shipping, and storage. No guidance is widely available to assist in the setting of these requirements, leading some manufacturers to use values that others have used, even though the packages may differ significantly in composition and application. Manufacturers would benefit from having access to strength data related to package characteristics and sealing process parameters as reference data for specifying seal-strength and seal-width requirements for a particular package.

Once the seal strength specification is set, the manufacturer has a new problem, which is developing a process that will consistently meet that specification. During the development of the sealing process, the device manufacturer determines the pressure and temperature that will be applied to the seal area, as well as the dwell time—the length of time temperature and pressure are applied. The strength of the resulting seal depends upon the particular tray material properties, lid material properties, adhesive properties, width of seal, and uniformity of the tray's flange area. There are currently no formulas that can be used to determine the seal strength that will result from a specified amount of change in one or more of these factors.

There are two types of tests generally used to evaluate seal strength for trays: tensile testing and burst testing. Tensile testing, also called peel testing, measures the force required to peel the seal apart. Burst testing measures the amount of internal pressure required to cause the seal to burst open. While tensile testing requires time consuming sample preparation and does not characterize the strength around the entire seal, burst testing is fast, requires no sample preparation, and tests the entire seal at once. Both tests give an indication of seal strength, but a general formula for the relationship between the two measures has not been established. Such a formula would encourage increased process monitoring in the safety-critical package sealing process through increased utilization of burst testing.

Package sealing processes for sterile products are required by the Quality System Regulation, 21 CFR Part 820, to be validated with a high degree of assurance. Validation means that there is a high degree of assurance that the process will consistently produce a product that meets its predetermined specifications. Companies routinely conduct process validation exercises and certify that the processes are validated. Nevertheless, there are failures of these "validated" processes every year, leading to recalls from the field. Figure 1 depicts the number of recalls for seal-related failures from February 20, 1990 to

December 31, 2007, and Figure 2 shows the quantities involved in these recalls. Over 10.4 million packages were recalled in 223 recalls. One packaging failure may lead to the injury or death of many people and can easily cost a company hundreds of thousands of dollars. As shown on the charts, the problem is not getting better, but seems to be getting worse. The causes of these failures lie in either a lack of information or deficient methodologies. Both of these areas need to be addressed for medical device trays.

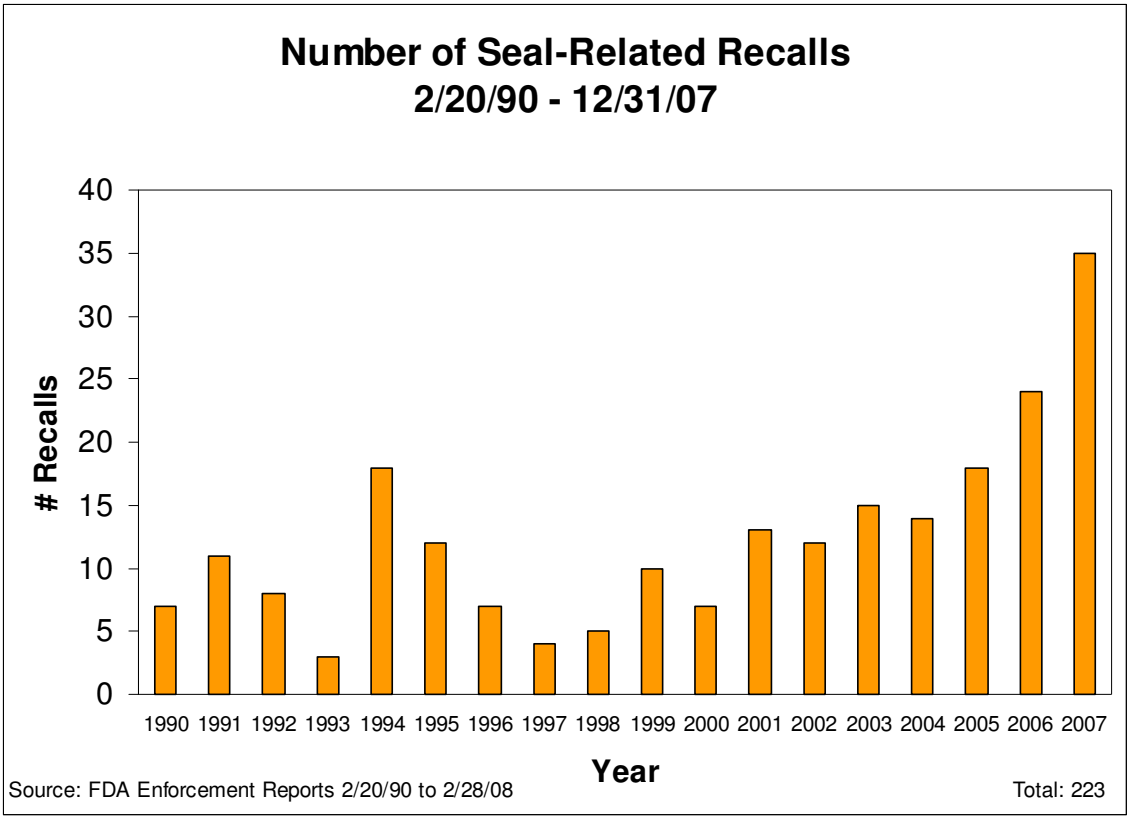

Figure 1. Number of seal-related recalls 2/20/90 to 12/31/07.

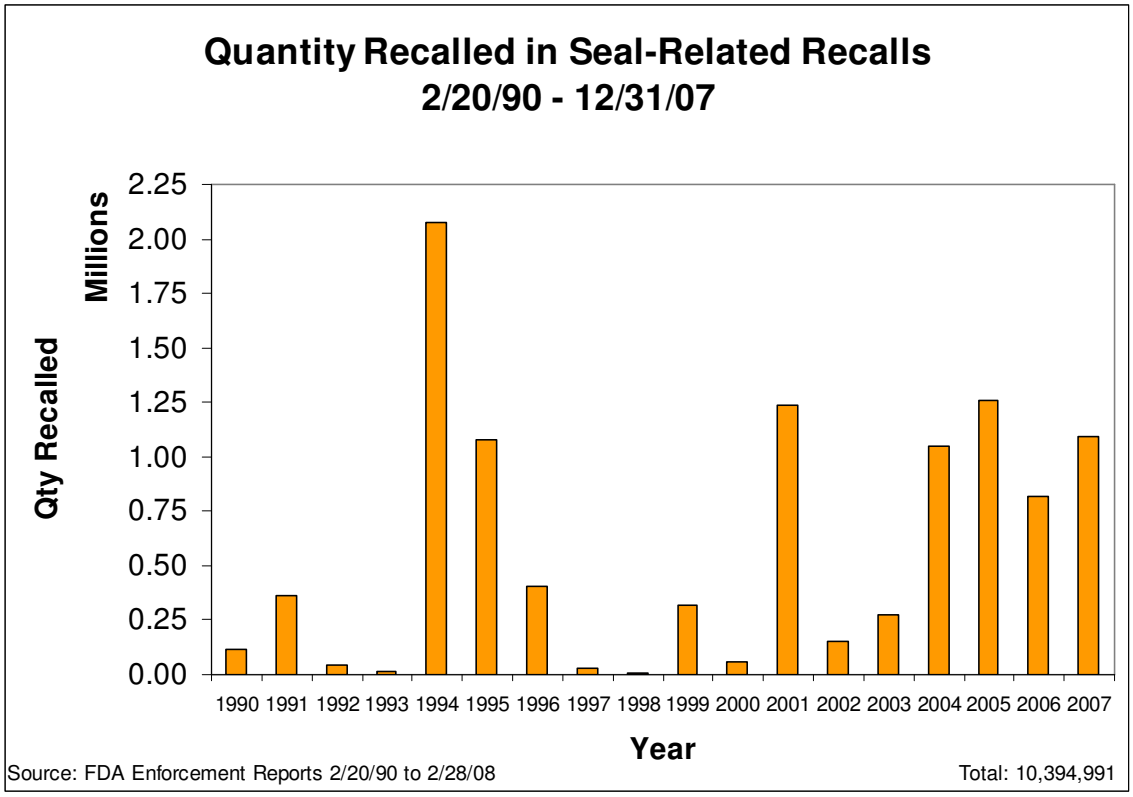

Figure 2. Quantity recalled in seal-related recalls 2/20/90 to 12/31/07.

Although several material and sealing process factors have been observed to affect peel force, the effects have not been quantified sufficiently to facilitate development of an equation describing the response. To date, there are no published data relating burst pressure directly to material and sealing process factors. Overall, there is a lack of published strength data related to package characteristics and sealing process parameters. Consequently, general formulas for the responses of peel force and burst pressure to combinations of material and process parameters have yet to be established. Mathematical models that allow prediction of tensile strength or burst pressure based on package composition and sealing process parameters would be useful during package design, sealing process development and validation, and ongoing manufacturing process control. Likewise, an improved methodology for preparing samples for testing would facilitate a better understanding of the relationship between the two types of seal strength tests and increase the effectiveness of all related package quality assurance processes.

Literature review

With the passage of the Medical Device Amendments to the Food, Drug, and Cosmetic Act in 1976, the Food and Drug Administration (FDA) was given oversight of medical devices. Under FDA oversight, medical device manufacturers began developing package testing methodologies in the early 1980's, but an emphasis on investigation of the science behind package testing issues did not begin until the mid 1990's.[1] The following review will first describe the current state of the knowledge in regard to factors affecting tensile seal strength (peel force) and inflation seal strength (burst pressure). Afterward, efforts to develop models of seal strength will be discussed.

The quality of the bond between a medical device tray and its lid is believed to be determined by the chemical properties of the tray, lid, and adhesive materials; cleanliness of the materials; width of the seal; uniformity of the tray flange, and the temperature, pressure, and dwell time settings of the heat seal machine. While it is plausible that all of these factors affect seal strength to varying degrees, neither the effects of each factor nor factor interaction effects have been adequately quantified. Both tensile test and burst test results are sensitive to changes in these factors, but the response relationships have not been established through generally applicable equations.

An experiment conducted by Franks and Barcan attempted to determine the sensitivity of the restrained burst test to sealing process changes by comparing the change in burst pressure to the change in tensile strength.[2] The sealing pressure parameter was held constant, temperature was tested at three levels, dwell time was tested at two levels, and restraining plate gap distance was tested at four levels. A linear regression plot showed a positive correlation between burst pressure and peel force, however, no regression equation was presented. The researchers concluded that the restrained burst test was able to identify the lowest seal-strength area for certain values of restraining plate gap distance. While the results indicated sensitivity of the burst test to process changes, the direct relationship between changes in burst pressure and sealing process factors was not established.

Franks reported that larger packages tend to burst at lower pressures, as do packages that are unrestrained and packages with peelable seals.[3] The observed burst pressure is further affected by the porosity of the package materials, seal type, geometry of the package, burst test equipment settings (pressure and flow rate), and the amount of restraint the package is under, in addition to the factors previously listed.[4] Porosity and flow rate are related, as the flow rate must compensate for the degree of porosity in order for enough air to fill the package to cause bursting.

There are a small number of published reports of efforts to quantify the effects of burst test parameters and package dimensions on burst pressure for pouches and very few reports of similar efforts for trays, as will be discussed below.

Franks and Barcan carried out a screening experiment to determine variables that may affect burst pressure.[2] The study used a restrained burst test to investigate the effects of length-to-width ratio and restraining plate gap on the burst pressure of nonporous pouches with peelable seals. The researchers also aimed to determine whether the burst area coincided with the lowest tensile-strength area and whether there was a difference in consistency between restrained and unrestrained burst tests. They found no significant effect of length-to-width ratio and no significant difference in variability between restrained and unrestrained burst tests. Gap distance was found to have a significant effect on burst pressure, with burst pressures varying inversely with gap distance. There was no indication that factor interactions were investigated.

Feliú-Báez, Lockhart and Burgess conducted a factorial experiment to investigate the effects of flow rate and plate separation on a restrained burst test for pouches and found that both plate gap and flow rate had a significant effect on burst pressure.[5]

A study by Feliú-Báez and Lockhart analyzed the effect of restraining plate separation values on restrained burst test results for pouches and trays.[6] Two different tray materials and one lid type were tested. Analysis of variance results showed that both gap size and tray perimeter measurement have inverse relationships with burst pressure, but there was no indication that the interaction of the two factors was investigated. The paper did not indicate that regression analysis had been performed using the data, and no equations relating burst pressure to gap size or tray dimensions were presented.

Efforts to develop models of seal strength have been limited. There are no published models that calculate burst pressure or peel force directly from given values of material and process factors. There is one published theoretical model developed by Yam, Rossen, and Wu and three empirical models published by Feliú-Báez, Lockhart, and Burgess that calculate burst pressure from a given peel force value for pouches.[5]

Yam, et al. developed a theoretical model based on force diagrams of pouches to predict the burst pressure associated with a given tensile strength. The resultant equation (P=2S/D) had only two independent terms, tensile seal strength (S) and restraining plate gap distance (D). The model requires that the time to peel the seal apart and the time to burst the seal be the same. Feliú-Báez, Lockhart and Burgess attempted to replicate Yam's experiment and found that the formula overestimated burst pressure, and the error varied with gap size.[7] This may have been due to differences in assumptions made, sampling techniques, and experimental method. Feliú-Báez, Lockhart and Burgess modified Yam's formula by adding a correction factor based on pouch length and width and found that the new model overestimated burst pressure more than the original model.[5]

After the force diagram approach failed to yield satisfactory results, Feliú-Báez, Lockhart, and Burgess used multiple-regression analysis to develop three empirical models relating restrained burst test pressures and peel forces for pouches.[5] The principal component of all three models is the term S/D, which has the same basic structure as the theoretical model. Other terms of the models included original package

length to width ratio, ratio of gap distance to inflated length, ratio of gap distance to inflated width, and the same correction factor that was applied to the theoretical model. These models were developed by relating average peel force for a group of pouches to average burst pressure for another group of pouches. The paper reported that all three models had strong positive correlation of burst pressure and seal strength with low error percentages, allowing either value to be calculated from the other. However, there was wide variation in regression coefficients for the same material type purchased from different suppliers. This indicates that there are factors that should be added to make the model useable over a range of applications.

In conclusion, the current body of published research that addresses seal strength testing for medical device trays includes a small number of studies with small sample sizes. A number of factors that may affect seal strength testing results have not been statistically analyzed, and interaction effects among study factors have typically not been quantified. A few theoretical and empirical models have been developed to relate burst pressure to peel force for pouches, but their universal applicability is limited by the assumptions required and the small number of factors accounted for. There have been no models developed for trays to relate burst pressure to peel force. Furthermore, there are no existing models that relate burst pressure and peel force directly to sealing process parameters.

CHAPTER II

A STRUCTURED METHODOLOGY FOR SAMPLE IDENTIFICATION FOR IMPROVED TEST DATA QUALITY

Background

Completion of peel testing of tray packages involves the cutting of strips from multiple locations around the perimeter of the tray. Commonly in the industry the specimen locations are selected haphazardly at the time of testing and are undocumented. Since specimens are not identified, there is no way to match data for a tested specimen to a specific location on the package. All specimens taken from a particular package are assumed to be homogeneous and are considered equally representative of the minimum peel force location of the tray. This assumption is not proven during process validation, however, this approach continues to be employed. There are several reasons that specimen locations should be considered unique entities and given unique identifiers.

One source of differentiation of specimen locations is the possibility of each location being subjected to different temperature or pressure during sealing depending upon the uniformity of the sealing tooling. If the tooling is not completely characterized and monitored, there could be unknown variations in temperature and pressure being applied at different tray locations.

Tray geometry is another source of distinction of tray specimens. Unlike pouches, trays have depth and typically multiple cavities which create various seal geometries. Each location may have different peel strength based on its specific geometry. The standard peel test method is based on a pull test with a pull force that is perpendicular to the seal. A seal that is angled or curved will create a different force profile than a straight seal.

A third source of specimen differentiation is the packaging materials themselves. Any inconsistencies in the lid stock or tray, or contaminants introduced to the seal area during processing may create different peel forces.

Identification of specimen locations would allow comparison of peel force values among locations within a tray and on different trays. This ability would help to identify patterns in observed seal strength, to characterize the strength of the whole package perimeter, and to monitor seal strength at each location.

Specimen identification also becomes important when attempting to relate burst pressure to seal strength. It is desirable to know the peel force at the location of burst in order to develop a true model of the relationship between burst pressure and peel strength. In order to maintain this traceability, a method of specimen identification is required. A structured methodology for specimen location identification was developed and employed in this research.

Methodology

A structured methodology for specimen location identification was developed and applied to increase the repeatability of testing the hundreds of packages in the study and to improve the accuracy of matching burst pressure samples to peel force samples. The methodology involved the development of custom templates for each package configuration using standard identifiers.

Template creation began with the identification and naming of specimen locations around the perimeter of a generic tray as shown in Figures 3 and 4. These would be the theoretical maximum number of locations on any tray. Each tray had a custom full template for burst location identification and a custom template with a subset of locations to be peel tested. The locations included on the peel test template depended on the observed burst locations and size and geometry of the particular tray. The research plan was designed to provide sets of matching packages for comparison of burst pressures to peel forces. In order to facilitate subsequent matching, burst testing was completed first to determine the burst location for each tray so that it could be ensured that a peel test specimen would be cut at the burst location of the matching tray. All observed burst locations were included in the template first, then side locations were added to total eight specimens if the tray size and geometry would accommodate them.

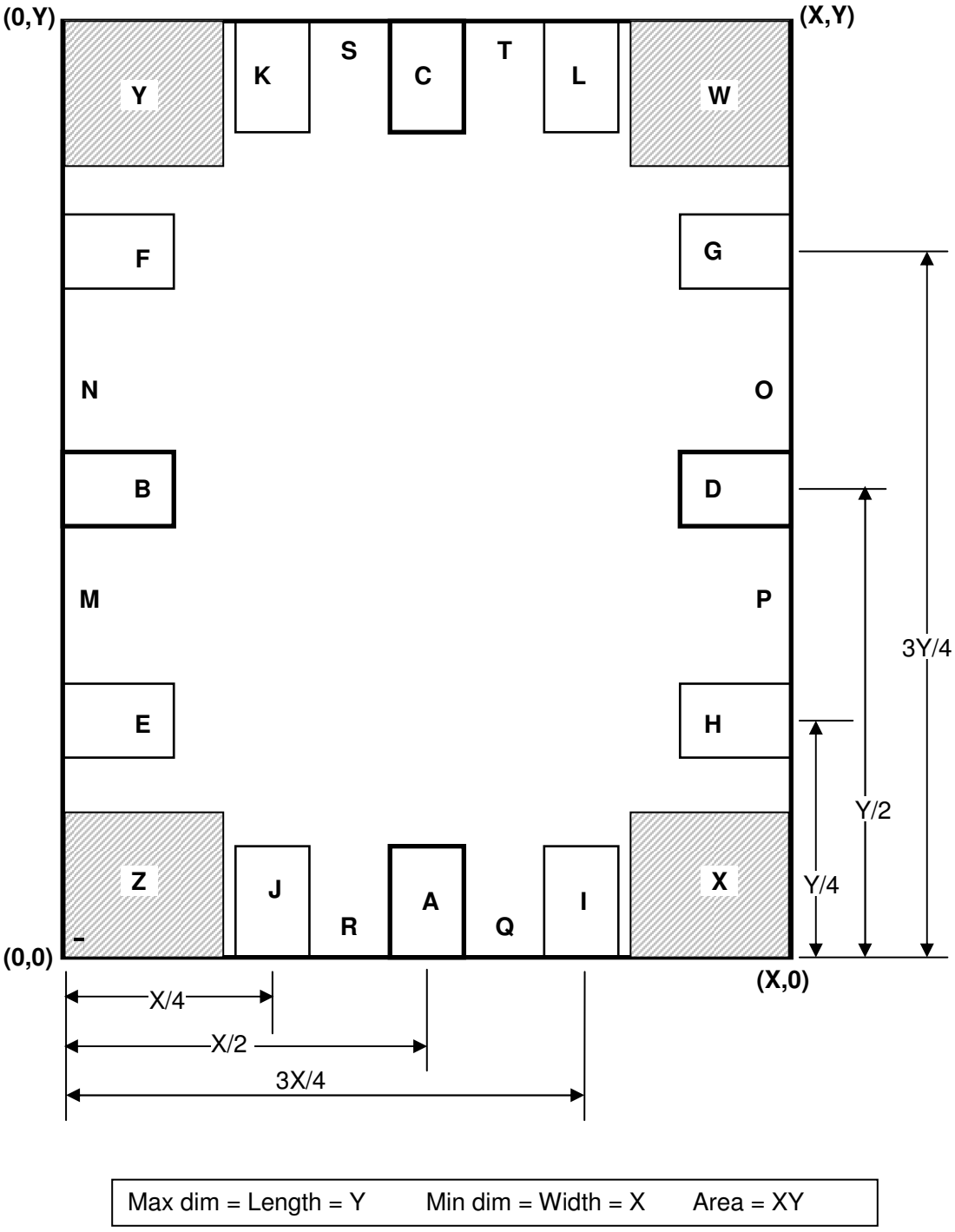

Figure 3. Generic tray diagram - vertical orientation.

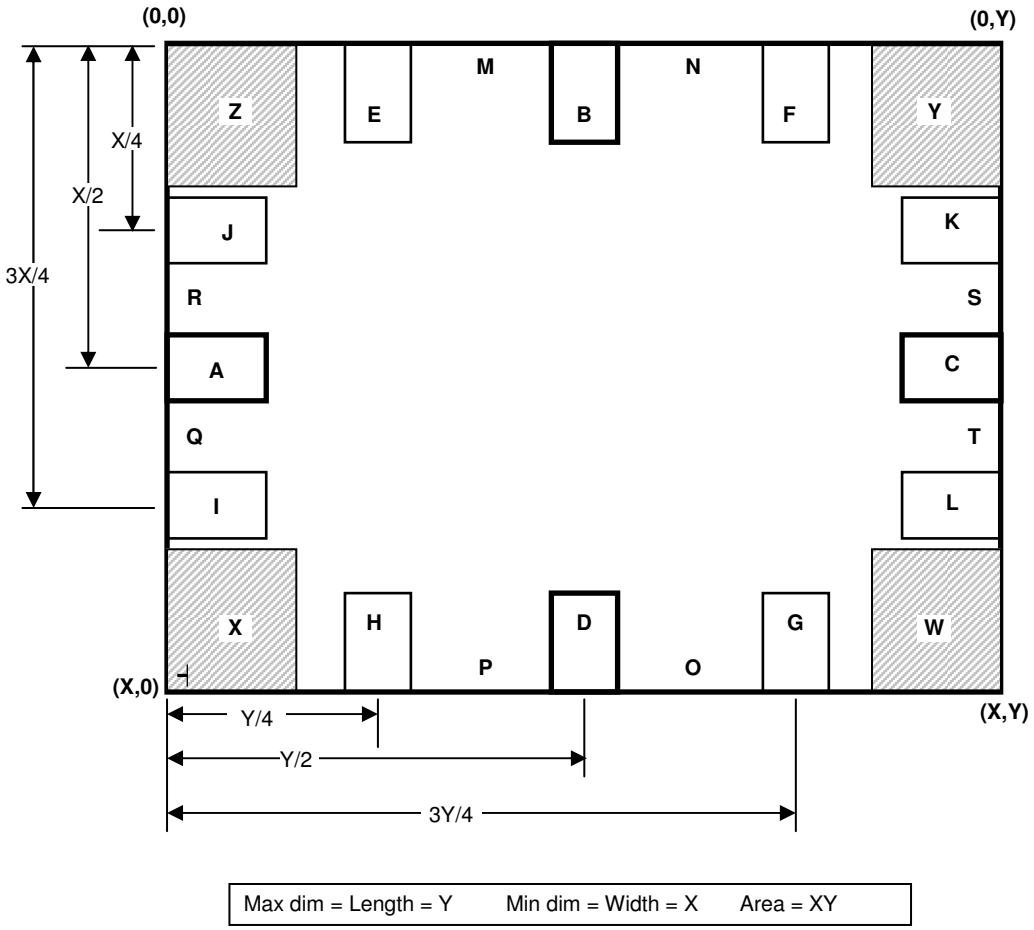

Figure 4. Generic tray diagram - horizontal orientation.

To begin creation of the templates, a plus sign was marked in one corner of the template paper. This corner would represent the front left corner of the tray as it was placed in the sealing cavity. This marker was used throughout sample identification to ensure that the templates were properly oriented for uniform specimen location identification on all packages. Next, the dimensions shown on the generic tray diagram were calculated for each tray based on the dimensions taken from the engineering drawing of the tray, and the midpoints of all the locations were marked on the template paper. Then 1-inch wide specimen outlines were drawn centered on those midpoints. For the peel test templates, the areas inside these 1-inch wide outlines were cut out to provide a tracing template. Diagrams for each tray showing the peel specimen locations are given in Appendix A1.

As trays were removed from the sealer, the front left corner was marked with a plus sign, to allow uniform orientation of the template for cutting peel test specimens and uniform orientation during burst testing. Each package was also identified with a package number. This package number concatenated with the specimen location comprised the specimen identifier for each specimen. Pairs of trays were sealed with identical parameters to be used for comparison of burst pressure with peel force. The specimen ID and package ID allowed one-to-one matching of the data for these samples.

In addition to specimen location, another piece of information was recorded for each specimen. As discussed above, it is possible that specimen geometry may affect observed peel force for the specimen. The specimens in the study had differing geometries depending on the locations and geometries of cavities in the tray, so the specimen geometries were classified into five categories as follows.

Category A specimens were the typical flat specimen with a seal perpendicular to the direction of pull, whose ends were rectangular and were able to be gripped flatly in the grips of the tester. Category B specimens also had a perpendicular seal, but due to the geometry of the package at the specimen locations, the area of the specimen that was held by the grips had a curved shape. Category C specimens had a diagonal seal with a rectangular gripping area, and Category D specimens had a diagonal seal with a curved gripping area. Category E specimens were the most uncommon, having a diagonal seal and diagonal gripping area.

The specimen identification methodology was used successfully to build, identify and test 440 packages. Several people were involved with the tray marking and specimen cutting, and the specimens were consistently produced. In addition, the identification of specimens provided the opportunity to perform several interesting analyses. For example, burst pressures were able to be matched exactly to specified peel specimens by ID number, histograms of burst location and lowest peel force locations were created, and percentages for matching of burst location to lowest peel force locations were calculated.

The use of a structured specimen identification methodology improves repeatability of testing, provides the capability to perform trending on seal strength by location, increases the capabilities for analyzing test data to uncover insights about package seal strength, and increases the accuracy of burst pressure to peel force comparison. These improvements in data quality may help to improve the quality of sealing process design and validation, resulting in fewer package failures.

CHAPTER III

EFFECT OF MEDICAL DEVICE TRAY CHARACTERISTICS AND PACKAGING PROCESS PARAMETERS ON PEEL FORCE

Experiment

Statement of the problem

Tensile seal-strength (peel force) values of lidded trays are affected by characteristics of the packaging materials and by parameters of the package sealing process. This experiment investigated the effects of sealing temperature, sealing pressure, and dwell time on tensile seal strength, as well as the difference in effects of two different sealing adhesives.

Response

The response studied in this experiment was peel force, the tensile force required to pull the seal apart, measured in Newtons (N).

Factors

The factors investigated were sealing pressure, dwell time, sealing temperature, and adhesive. The factors controlled were tray material and lid material. Seal width was measured but not controlled, because it is determined by hard tooling which cannot be varied in the manner required to complete a factorial experiment.

Research and discussions with medical device packaging industry leaders identified the range of several package characteristics that would encompass a wide range of medical device packages that are in use and expected to be in use during the upcoming years. Packages were sought and selected into the study to reflect these characteristics, in order to give the developed models broader applicability. Specifically, PETG was selected as the tray material, as it is used predominately by manufacturers of high-end medical devices. For the same reason, the lid stock selected was Tyvek 1073B. The two water-based adhesives selected are the most popular for their respective manufacturers.

Nine trays of various areas, volumes and length-to-width ratios were sealed with 27 different combinations of seal pressure, seal temperature, and dwell time. Trays were selected to yield three levels of area and three levels of length-to-width ratio. The minimum and maximum seal process settings were selected to cover the range of values for these settings that are likely to be used in the industry.

Factor descriptions and types, number of levels, units of measure, and effect types are given in Table 1.

Table 1. Peel force experiment factors

Factor	Description	UOM	Factor Type	Levels	Effect Type
SealPressure	Pressure applied to join lid to tray	psi	Quantitative	75 / 85 / 95	Random
DwellTime	Amount of time pressure is applied at a temperature high enough to activate the adhesive	sec	Quantitative	3 / 4.5 / 6.5	Random
SealTemp	Temperature applied to join lid to tray	F	Quantitative	240 / 260 / 290	Random
Adhesive	Bonding agent applied to lid	N/A	Qualitative	2635B / CR-27	Fixed
TrayMaterial	Plastic from which tray is formed	N/A	Qualitative	PETG	Fixed
LidMaterial	Lid stock from which lid is cut	N/A	Qualitative	Tyvek 1073B	Fixed

Materials

Nine tray configurations were used in the experiment, as described in Table 2. The trays were sealed with Tyvek 1073B lids coated with Amcor 2635B or Perfecseal CR-27 adhesive.

Table 2. Tray configurations

Package	Tray Material	Tray Length (in.)	Tray Width (.in)	Tray Height (in.)	Tray Volume (fl oz)	Length-Width Ratio	Tray Area (sq in.)	Seal Width (in.)	Seal Perimeter (in.)
PS1	PETG .030	5.5	4.9	1.03	12.0	1.1	26.9	0.27	18.6
PS2	PETG .030	9.7	5.7	0.8	10.0	1.7	55.5	0.342	27.5
PS3	PETG Glidex .035	16.7	3.4	1.65	18.0	4.9	56.9	0.45	36.3
PS4	PETG .030	9.8	7.8	1.625	20.0	1.3	76.8	0.345	32.0
PS5	PETG Glidex .040	13.9	4.3	1.1	14.0	3.2	60.0	0.42	32.9
PS6	PETG Glidex .035	18.7	3.4	1.65	22.0	5.5	63.8	0.45	40.3
PS7	PETG .030	15.6	9.9	1.25	42.0	1.6	153.4	0.6	45.6
PS8	PETG .035	20.5	9.8	1.69	64.0	2.1	201.5	0.375	55.8
PS9	PETG Glidex .045	17.6	4.8	3	52.0	3.7	84.1	0.45	40.7

Methods

Packages were heat sealed and then inspected according to the F1886-98 standard for visual inspection of medical package seals. [8] The locations of all voids, overheated areas and flange deformation were recorded using code 1 for voids, code 2 for overheating, and code 3 for flange deformation.

The sealed packages were peel tested according to the F88-07 seal strength testing standard.[9] Up to eight 25.4 mm (1 in.) wide by 50.8 mm (2 in.) long peel test specimens were cut from each tray, depending on tray size. Diagrams for the nine trays, illustrating the specimen locations, are shown in Appendix A1. The + on each diagram indicates the left front corner of the tray, as it was loaded into the heat sealer. Table 3 indicates the locations at which specimens were cut for each package.

The sealing equipment, tensile test equipment, and experimental conditions for each package are given in Table 3. Tray specimens were loaded with the tray component clamped into the upper grip, the Tyvek component clamped into the lower grip, and the tail unsupported. Figure 5 shows the tensile test equipment with a tray specimen loaded into the tensile tester. The specimens were peel tested at 304.8 mm/min (12 in./min) with an initial grip separation of 25.4 mm (1 in.). The failure mode and peak peel

force for each specimen were recorded, and all raw data were saved for subsequent calculation of average peel force.

Table 3. Peel force experimental conditions

Package	Sealer	Room Temp (C)	RH %	Specimens	Load Frame	Load cell	Load Cell Capacity	Room Temp (C)	RH %
PS1	Alloyd 2S1428 #02	22	50	A B C D W X Y Z	Shimadzu Autograph AG-IS	Shimadzu 346-52114-04	50N	23	50
PS2	Alloyd 2S1428 #02	22	50	B C D G W X Y Z	Shimadzu Autograph AG-IS	Shimadzu 346-52114-04	50N	23	50
PS3	Alloyd 2S1428 #03	22	50	E HP M W X Y Z	Shimadzu Autograph AG-IS	Shimadzu 346-52114-04	50N	23	50
PS4	Alloyd 2S1428 #02	22	50	A B D J W X YK	Shimadzu Autograph AG-IS	Shimadzu 346-52114-04	50N	23	50
PS5	Alloyd 2SM1428 #01	22	50	E F G H W X Y Z	Shimadzu Autograph AG-IS	Shimadzu 346-52114-04	50N	23	50
PS6	Alloyd 2S1428 #03	22	50	E F OG N W X Y Z	Shimadzu Autograph AG-IS	Shimadzu 346-52114-04	50N	23	50
PS7	Alloyd 2S1428 #02	22	50	F H J L W X Y Z	Shimadzu Autograph AG-IS	Shimadzu 346-52114-04	50N	23	50
PS8	Alloyd 2SM1428 #04	21	48	A B C D W X Y Z	Instron 5544	Instron 2530-427	100N	23	50
PS9	Belco BM2020 #05	22	50	E F G H W X Y Z	Shimadzu Autograph AG-IS	Shimadzu 346-52114-04	50N	23	50

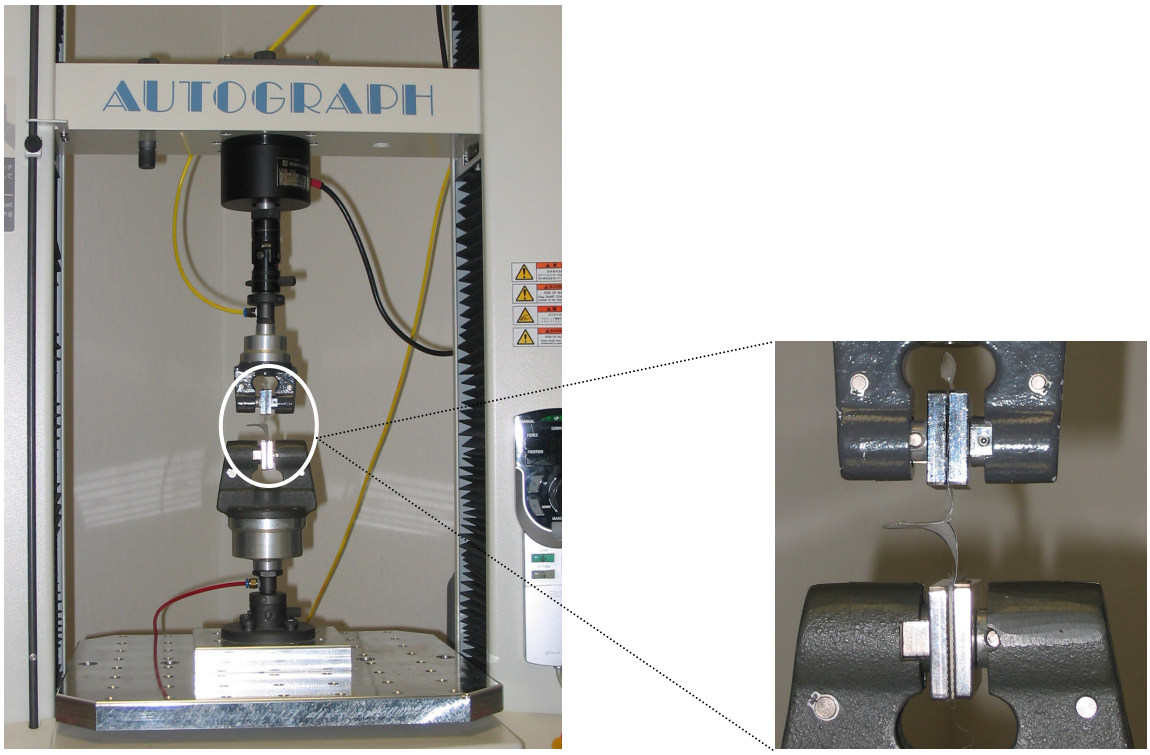

Figure 5. Tensile test equipment with specimen loaded.

Design

Design selection

To study the peel force response to SealTemp, SealPressure, and DwellTime, a face-centered central composite design with 17 runs as defined in Table 4, was used.

To study the peel force response to Adhesive, the 17 runs of the central composite design were run at the two levels of Adhesive with one package (PS8).

Replication

Nine replicates of the experiment were run, with Adhesive varied in replicate one only. In replicates two through eight, Adhesive was fixed at 2635B only.

Data from all nine replicates were analyzed to investigate the effect of SealTemp, SealPressure, and DwellTime. The sample size for this data set was 153 (9 replicates x 17 runs).

Data from replicate one were analyzed to investigate the effect of Adhesive. The sample size for this data set was 34 (1 replicate x 34 runs).

Table 4. Peel force central composite design runs

SealTemp	SealPressure	DwellTime	Point Description	Point Number
260	75	4.5	FrontFace	1
260	95	4.5	BackFace	2
240	85	4.5	LeftFace	3
290	85	4.5	RightFace	4
260	85	3	BottomFace	5
260	85	6.5	TopFace	6
240	75	3	Corner	7
240	75	6.5	Corner	8
240	95	3	Corner	9
240	95	6.5	Corner	10
290	75	3	Corner	11
290	75	6.5	Corner	12
290	95	3	Corner	13
290	95	6.5	Corner	14
260	85	4.5	Center	15
260	85	4.5	Center	16
260	85	4.5	Center	17

Randomization

After each change in seal temperature, the sealing equipment had to stabilize for at least 20 minutes. Sealer pressure also had to be stabilized after each change by cycling the sealer platen two or three times and readjusting the pressure control valve until the desired pressure was set and stable. Due to the length of time required to change seal temperature and seal pressure, runs were not completely randomized. A split-split-plot design, illustrated in Figure 6, was used to complete the runs, with temperature in the whole plot, pressure in the subplot, and dwell time and adhesive randomized within the subplot. The order of the whole plots was random, as was the order of the subplots within each whole plot.

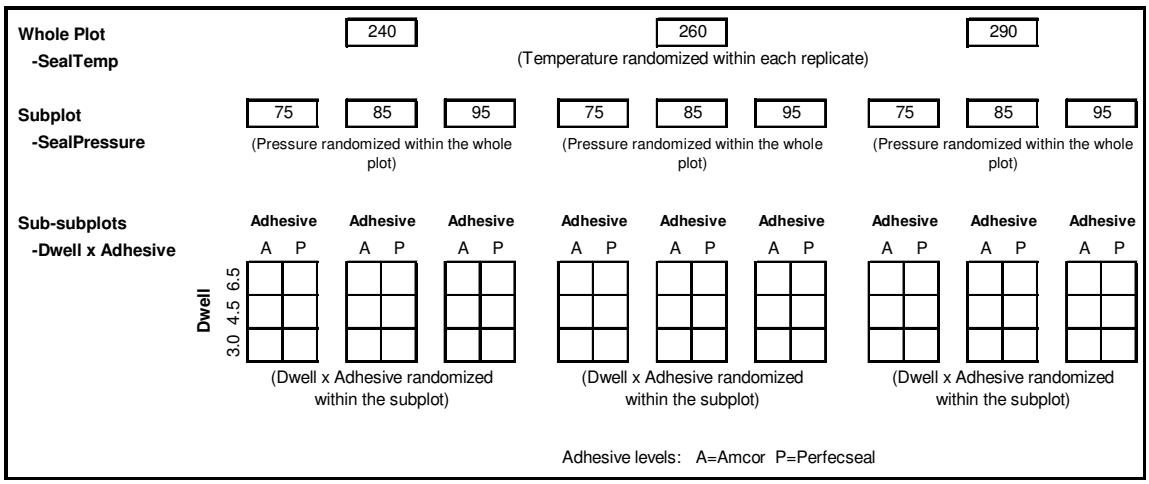

Figure 6. Split-split-plot design for peel force.

Blocking

The central composite design was replicated for each of the nine package configurations. Due to potential effects of differences in package geometries, Package was treated as a blocking variable.

Statistical models

The linear statistical model for the split-split-plot design to study the effect of Adhesive is

$$y_{jklm} = \mu + \beta_j + \gamma_k + (\beta\gamma)_{jk} + \delta_l + (\beta\delta)_{jl} + (\gamma\delta)_{kl} + (\beta\gamma\delta)_{jkl} + \lambda_m + (\beta\lambda)_{jm} + (\gamma\lambda)_{km} + (\delta\lambda)_{lm}$$
$$+ (\beta\gamma\lambda)_{jkm} + (\beta\delta\lambda)_{jlm} + (\gamma\delta\lambda)_{klm}$$
$$+ (\beta\gamma\delta\lambda)_{jklm} + \varepsilon_{jklm} \qquad \begin{cases} j = 1, 2, 3 & \text{(SealTemp)} \\ k = 1, 2, 3 & \text{(SealPressure)} \\ l = 1, 2, 3 & \text{(DwellTime)} \\ m = 1, 2 & \text{(Adhesive)} \end{cases} \qquad (3.1)$$

where the effects in the model correspond to the study factors as listed in Table 5.

The linear statistical model for the split-split-plot design to study the effect of SealTemp, SealPressure, and DwellTime is

$$y_{ijkl} = \mu + \tau_i + \beta_j + (\tau\beta)_{ij} + \gamma_k + (\tau\gamma)_{ik} + (\beta\gamma)_{jk} + (\tau\beta\gamma)_{ijk} + \delta_l + (\tau\delta)_{il} + (\beta\delta)_{jl} + (\tau\beta\delta)_{ijl} + (\gamma\delta)_{kl} + (\tau\gamma\delta)_{ikl} + (\beta\gamma\delta)_{jkl} + (\tau\beta\gamma\delta)_{ijkl} + \varepsilon_{ijkl} \qquad \begin{cases} i = 1, 2, \ldots, 9 & \text{(Replicates)} \\ j = 1, 2, 3 & \text{(SealTemp)} \\ k = 1, 2, 3 & \text{(SealPressure)} \\ l = 1, 2, 3 & \text{(DwellTime)} \end{cases} \tag{3.2}$$

where the effects in the model correspond to the study factors as listed in Table 6.

Table 5. Factor effects for the split-split-plot design for studying effect of adhesive on peel force

Element	Factor	Effect
Whole plot	SealTemp main effect	β_j
Subplot	SealPressure main effect	γ_k
	SealTemp x SealPressure interaction (Subplot error)	$(\beta\gamma)_{jk}$
Sub-subplot	DwellTime main effect	δ_l
	SealTemp x DwellTime interaction	$(\beta\delta)_{jl}$
	SealPressure x DwellTime interaction	$(\gamma\delta)_{kl}$
	SealTemp x SealPressure x DwellTime interaction	$(\beta\gamma\delta)_{jkl}$
	Adhesive main effect	λ_m
	SealTemp x Adhesive interaction	$(\beta\lambda)_{jm}$
	SealPressure x Adhesive interaction	$(\gamma\lambda)_{km}$
	DwellTime x Adhesive interaction	$(\delta\lambda)_{lm}$
	SealTemp x SealPressure x Adhesive interaction	$(\beta\gamma\lambda)_{jkm}$
	SealTemp x DwellTime x Adhesive interaction	$(\beta\delta\lambda)_{jlm}$
	SealPressure x DwellTime x Adhesive interaction	$(\gamma\delta\lambda)_{klm}$
	SealTemp x SealPressure x DwellTime x Adhesive (Sub-subplot error)	$(\beta\gamma\delta\lambda)_{jklm}$

Table 6. Factor effects for the split-split-plot design for studying effect of seal process parameters on peel force

Element	Factor	Effect
Whole plot	Replicates (Packages or blocks)	τ_i
	SealTemp main effect	β_j
	Whole plot error (Replicates x SealTemp)	$(\tau\beta)_{ij}$
Subplot	SealPressure main effect	γ_k
	Replicates x SealPressure interaction	$(\tau\gamma)_{ik}$
	SealTemp x SealPressure interaction	$(\beta\gamma)_{jk}$
	Subplot error (Replicates x SealTemp x SealPressure)	$(\tau\beta\gamma)_{ijk}$
Sub-subplot	DwellTime main effect	δ_l
	Replicates x DwellTime interaction	$(\tau\delta)_{il}$
	SealTemp x DwellTime interaction	$(\beta\delta)_{jl}$
	Replicates x SealTemp x DwellTime interaction	$(\tau\beta\delta)_{ijl}$
	SealPressure x DwellTime interaction	$(\gamma\delta)_{kl}$
	Replicates x SealPressure x DwellTime interaction	$(\tau\gamma\delta)_{ikl}$
	SealTemp x SealPressure x DwellTime interaction	$(\beta\gamma\delta)_{jkl}$
	Replicates x SealTemp x SealPressure x DwellTime (Sub-subplot error)	$(\tau\beta\gamma\delta)_{ijkl}$

Analysis

Data collection and processing

The central composite design for studying peel force response to SealTemp, SealPressure, and DwellTime was replicated nine times. The 290° setting proved to be infeasible for five of the trays (PS1, PS2, PS4, PS7, PS9) as the flanges tended to melt at this temperature. This was most likely due to smaller wall thicknesses created during thermoforming. As a result, there were five missing data points for each of these five trays, yielding 128 packages in the sample instead of 153.

An additional 17 trays were sealed for package PS8 with the CR27 adhesive for evaluation of the effect of Adhesive, yielding a total of 145 packages for peel testing.

Several specimens were cut from each package, as shown in Table 3, and identified according to the methodology described in Chapter II. Each specimen was peel tested in random order, peak peel force was recorded, the force profile was saved, and the raw data were exported for subsequent analysis.

Average peel force was calculated from the raw data by excluding forces less than or equal to 0.3 N and averaging the data points within the central 80% of the remaining force profile. In the industry, the peak peel force measure may be used more commonly than average peel force since it requires less data processing. A significant difference between peak and average peel force measures in terms of variability or performance could have practical significance for package testers. Therefore, analyses involving peel force were performed with both peak peel force and average peel force, and comparisons were made of the variability between the two measures and the conclusions reached using the two measures.

Different geometries of specimens might be expected to create different force profiles when peel tested, so uniformity of the peel force means and variances at the different specimen locations and among specimen categories was evaluated using histograms and box plots.

Descriptive statistics and graphical analysis

Numerous tables and graphs were produced to summarize the specimen data and aid in the identification of patterns in the data. These analyses are included in several separate appendices.

A total of 145 packages were used in the peel test study. 1131 specimens were cut from these trays, at 19 specimen locations. Table A2-1 in Appendix A2 and Table A15-1 in Appendix A15 summarize the study specimens, showing quantities by Package, Specimen Location, and Specimen Category.

Table A2-2 in Appendix A2 shows the number of packages and number of specimens, as well as mean, standard deviation, minimum and maximum of peak peel force for each Point Number, grouped by Adhesive for comparison. Table A15-2 in Appendix A15 presents the corresponding information for average peel force. Seal process settings for each Point Number are as defined in Table 4.

Table A2-3 in Appendix A2 shows the number of specimens, as well as mean, standard deviation, minimum and maximum of peak peel force for each sealed package, grouped by Point Number and Adhesive for comparison. Table A15-3 in Appendix A15 presents the corresponding information for average peel force.

Table A2-4 in Appendix A2 gives mean and standard deviation of peak peel force for the specimens from each sealed package. The lowest peel force location for each package is identified by an asterisk. Table A15-4 in Appendix A15 presents the corresponding information for average peel force. (Note: 19 specimens were not peel tested because they separated prior to peel testing due to negligible seal strength. Zero values were entered for the peak and average forces for these specimens.)

Appendix A3 includes peel test force profiles for all specimens, grouped by Adhesive, Package and Specimen Location. Each plot is annotated with the peak and average peel force. A review of the force profiles indicates that average peel force was lower than peak peel force for all specimens peeled. Figure 7 displays a histogram of the difference of peak force over average force. The minimum percent difference was 4.64% and the maximum percent difference was 335.16%.

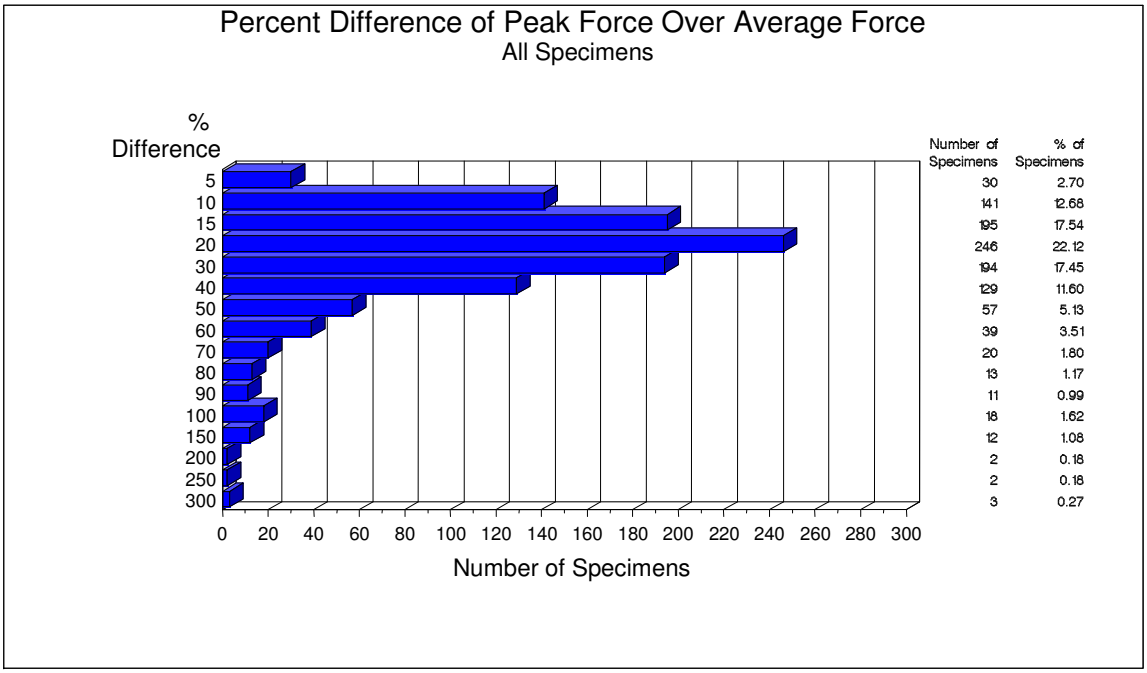

Figure 7. Percent difference of peak force over average force.

The grouping of force profiles provided in Appendix A3 facilitates comparison of the profiles for specimens at each location on each package. As an example, force profiles for four specimens from package PS5 are shown in Figure 8.

Figure 8. Example force profiles grouped by adhesive, package and point number.

Force profiles were reviewed to identify the typical shape for each specimen category and location. In general, the specimens of category A have an inverted bathtub-shaped profile, with some mountain-shaped profiles. In general, category B specimens have a mountain-shaped profile, with some inverted bathtub-shaped profiles. In general, categories C, D, and E specimens have a mountain-shaped profile. With a few exceptions, summarized in Table 7, profile shapes are consistent within each location, across all process settings and across all packages. Based on a review of the graphs and this table, the exceptions to uniform profiles seem to be related to the effects of process settings (point number) rather than specimen location. The PS8 package had more exceptional force profiles than the other packages. This was probably because the PS8 package/sealer combination required relatively high temperature/dwell time settings to produce a uniform seal, and most of the temperature/dwell time settings studied were more moderate.

Table 7. Peel force profile exceptions

Specimen Category	Package	Specimen Location	Specimen ID (Amcor)	Point Number (Amcor)	Specimen ID (Perfecseal)	Point Number (Perfecseal)
B	PS1	X	1745X	2	N/A	N/A
B	PS1	X	1752X	8	N/A	N/A
B	PS1	Y	1733Y	5	N/A	N/A
A	PS2	B	1784B	7	N/A	N/A
A	PS2	Z	1784Z	7	N/A	N/A
A	PS3	E	1819E	7	N/A	N/A
A	PS3	M	1826M	9	N/A	N/A
A	PS3	W	1826W	9	N/A	N/A
A	PS3	X	1826X	9	N/A	N/A
A	PS3	Y	1826Y	9	N/A	N/A
B	PS7	W	1945W	6	N/A	N/A
A	PS8	A	3001A-3011A, 3013A & 3015A, 3016A, 3017A	1-11, 13, 15, 16, 17	3018A-3022A, 3024A, 3026A, 3028A, and 3034A	1-5, 7, 9, 11, 17
A	PS8	B	3001B, 3003B, 3005B, 3007B, 3013B, 3016B	1, 3, 5, 7, 13, 16	3018B, 3028B, 3030B, 3032B-3034B	1, 11, 13, 15-17
A	PS8	C	3005C, 3007C, 3009C	5, 7, 9	3022C, 3024C, 3026C	5, 7, 9
A	PS8	D	3001D, 3003D, 3005D, 3007D, 3009D, 3013D	1, 3, 5, 7, 9, 13	3018D-3020D, 3024D, 3030D, 3033D	1-3, 7, 13, 16
A	PS8	W	3007W	7	3022W, 3024W	5, 7
A	PS8	X	3001X-3007X, 3009X-3011X, 3013X, 1037X, 3017X	1-7, 9-11, 13, 15, 17	3018X, 3020X-3025X, 3027X, 3028X, 3030X, 3032X, 3033X	1, 3-7, 8, 10, 11, 13, 15, 16
A	PS8	Y	3005Y, 3009Y	5, 9	3022Y, 3026Y	5, 9
A	PS8	Z	3005Z, 3010Z, 3011Z, 3013Z, 3017Z	5, 10, 11, 13, 17	3018Z, 3020Z, 3025Z, 3028Z, 3032Z, 3033Z	1, 3, 8, 11, 15, 16

Appendix A4 includes peel test force profiles for all specimens, grouped by Adhesive, Point Number and Specimen Category. This grouping facilitates comparison of force profiles for specimens that were sealed with the same process parameters and have the same basic geometry. Each plot is annotated with the peak and average peel force. Force profile shapes were seen to be consistent for packages within each point number/specimen category combination, with the exception of PS8 specimens. This was because higher temperature/dwell time settings were required to produce a uniform seal for the PS8 package.

The force profiles from Appendix A4 are summarized by box plots comparing peak and average peel forces for packages by Adhesive, Point Number, and Category; these plots are presented in Appendix A5 in two sections. Section 1 of Appendix A5 includes box plots that compare forces for packages by Adhesive, Point Number, and Category. Section 2 includes box plots comparing Adhesive/Point Number/Category groups across all packages. The boxes in the box plots were defined by the interquartile range (IQR=75%ile-25%ile) of the response, with an upper fence at 75%ile + 1.5*IQR, a lower fence at 25%ile - 1.5*IQR, and outliers falling outside of the upper or lower fence.

The box plots in Section 1 showed that forces were consistent across packages for certain seal settings and specimen categories. For example, Point Number 6 equates to a temperature of 260ºF, pressure of 85 psi, and dwell time of 6.5 seconds. This setting with the Amcor adhesive resulted in mean average peel forces of about 4.5N to about 5.5N for category A and B specimens for all packages except PS8. The variances were also consistent across the eight packages at this setting. The box plots for this case are shown in Figure 9. Specimen categories D and E displayed the lowest peel forces; category C specimens had higher forces than category D and E specimens, but lower forces than category A and B specimens.

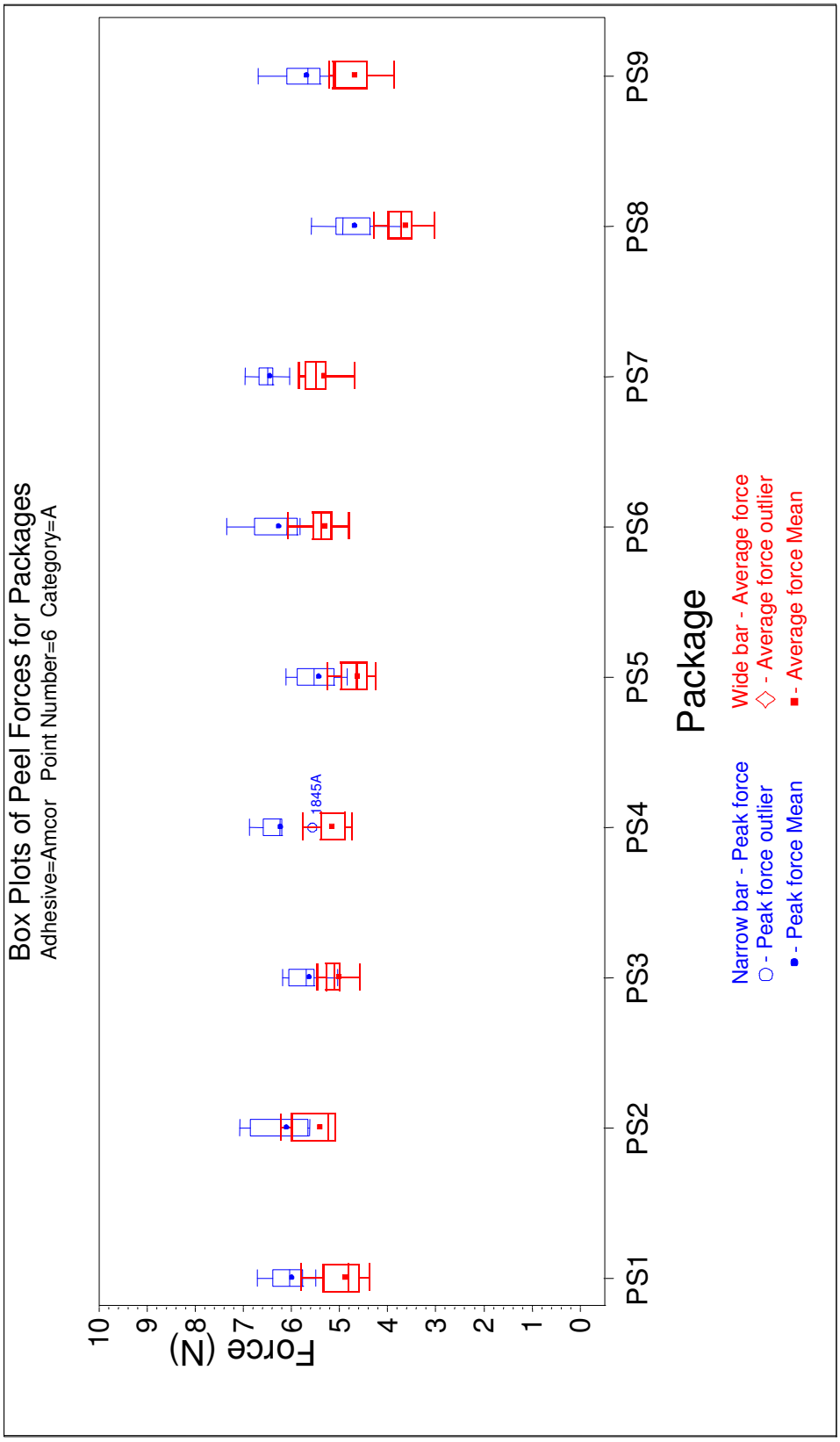

Figure 9. Example box plot of peel forces for packages by adhesive, point number and category.

Appendix A6 includes plots of peak force at each specimen location on each sealed package, grouped by Package. This grouping facilitates evaluation of the consistency—within a specific package configuration—of the relative peel force values for specimen locations, across seal process settings. That is, it allows one to evaluate whether the ranking of specimen locations varies based on the seal process settings (Point Number). Each plot is annotated with the mean, standard deviation, minimum and maximum of peak peel force, as well as ±3 standard deviations reference lines and number of specimens in the sample. Appendix A16 includes the corresponding plots of average force. The plots indicate that the process settings affect the ranking of specimen locations by peel strength, although the rankings are fairly consistent across the process settings.

Appendix A7 includes plots of peak force at each specimen location on each sealed package, grouped by Point Number. This grouping facilitates evaluation of the consistency—within a specific seal process setting—of the relative peel force values for specimen locations, across package configuration. That is, it allows one to evaluate whether the ranking of peel force for specimen locations varies by package. Each plot is annotated with the mean, standard deviation, minimum and maximum of peak peel force, as well as ±3 standard deviations reference lines and number of specimens in the sample. Appendix A17 includes the corresponding plots of average force.

The plots in Appendix A7 and A17 are summarized by box plots comparing peak peel force and average peel force for Packages and Specimen Locations, by Adhesive and Point Number; these plots are presented in Appendix A8. Section 1 of Appendix A8 includes box plots that compare forces for packages by Adhesive and Point Number. Section 2 includes box plots comparing forces for specimen locations across all packages by Adhesive and Point Number.

The box plots in Section 1 showed more variability in peel forces than the box plots by specimen category, due to the variation in peel force around the tray perimeter. However, it was still evident that certain seal settings could be identified that would produce consistent peel forces across packages, such as Point Number 6 and Point Numbers 15-17 (temperature 260ºF, pressure 85 psi, dwell time 4.5 s). The box plots for Point Number 15 are shown in Figure 10.

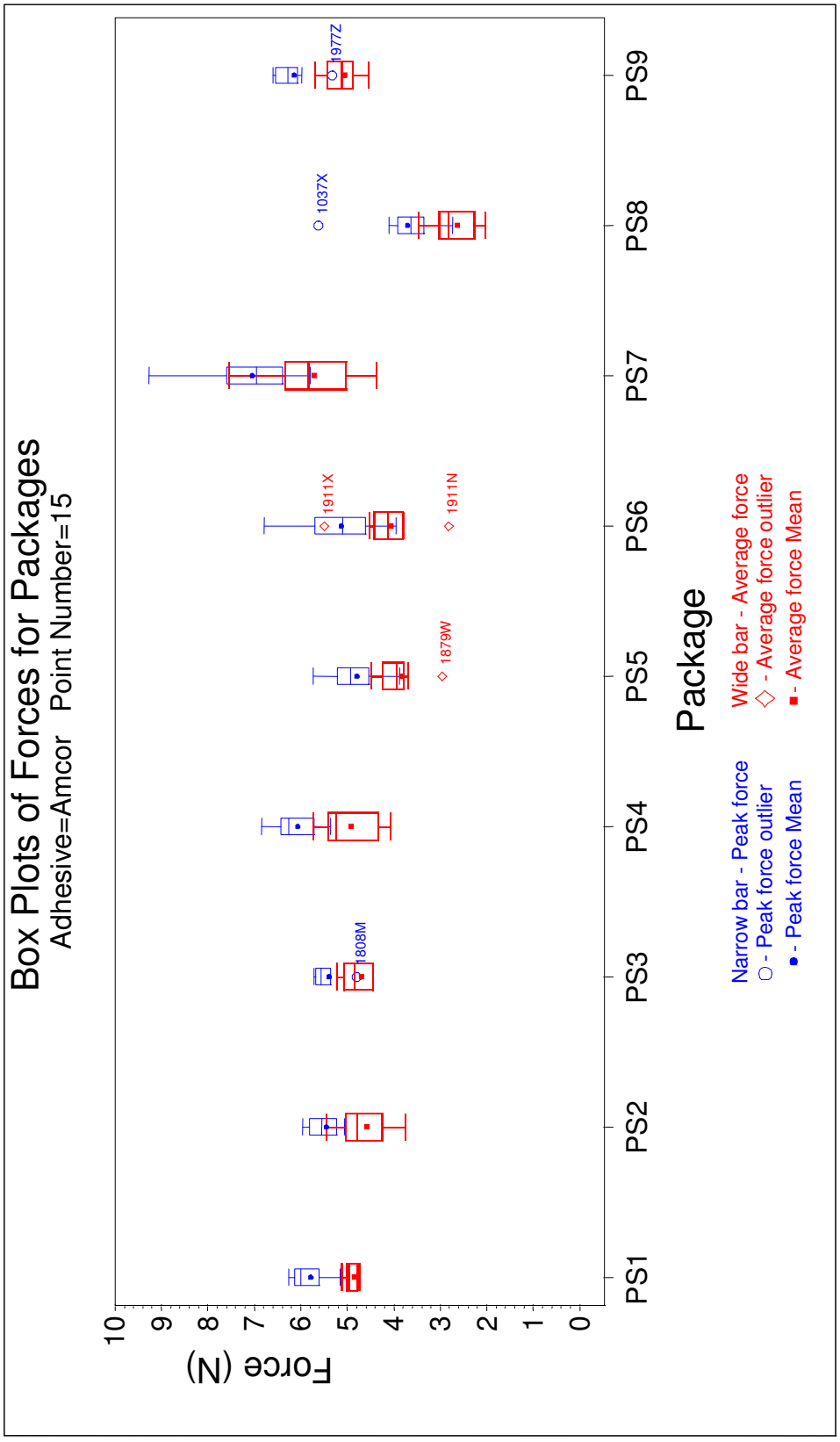

Figure 10. Example box plot of peel forces for packages by adhesive and point number.

Appendix A9 includes a histogram of lowest peak force location across all specimens. Appendix A18 includes the corresponding histogram of lowest average force location. Specimen location ‘Z’ was the location of lowest peak peel force for about 17% of packages, followed by location ‘X’ at about 14%, location ‘W’ at about 13%, and location ‘Y’ at about 7%. These locations are the four corner locations of all packages. The average force histograms reveal similar results. Specifically, specimen location ‘X’ was the location of lowest average peel force for about 20% of packages, followed by location ‘Z’ at about 14%, location ‘W’ at about 11%, location ‘N’ at about 7%, and location ‘Y’ at about 7%. (Location N is near corner ‘Y’).

Appendix A10 includes histograms of lowest peak force location grouped by Package and Adhesive. This grouping facilitates identification of patterns in lowest peel force location for a specific package geometry sealed with various seal process settings. Appendix A19 includes the corresponding histograms of lowest average force location. Six of nine packages had a corner location as the most frequent location of lowest peak peel force. Eight of nine packages had a corner location as the first or second most frequent lowest peak peel force location, and all nine packages had at least one corner location ranking first, second, or third. Similar results were seen for lowest average force, for which seven of nine packages had a corner location as the most frequent lowest average force location.

Appendix A11 includes histograms of lowest peak force location grouped by Point Number and Adhesive. This grouping facilitates identification of patterns in lowest peel force location for all packages sealed with common seal process settings. Appendix A20 includes the corresponding histograms of lowest average force location. Sixteen of seventeen process settings resulted in a corner location being the most frequent location of lowest peak peel force, and all seventeen process settings resulted in at least one corner location ranking first or second. The lowest average force histograms showed that sixteen process settings resulted in a corner location as the most frequent lowest average force location.

The observations drawn from the histograms indicate that across all process settings and package configurations, one of the corners of the package can be expected to exhibit the lowest peel force. Traditionally, peel test specimens are not taken from areas near the corners of trays. Rather, they are cut from the central portions of the sides—away from the corners. If the lowest peel force location is truly near one of the corners, the peel test results obtained using centrally located specimens may be overestimating the minimum peel force of the package.

Regression analysis

The data from this experiment were used to fit linear models of peel force response to sealing process factors. This analysis is described in Chapter IV.

Analysis of effect of adhesive

The central composite design for studying the effect of Adhesive on peel force was unreplicated, so the adhesive effect was analyzed using normal probability plots and plots of residuals. There were 272 specimens from 34 packages of configuration PS8 in the sample. Since the multiple specimens represent repeated measurements on one package, the average of the specimen peel force values was used as the response for the analysis. An initial regression was performed for the peel force response on a full model including all main effects and interactions for seal temperature, seal pressure, dwell time, and adhesive. The effects from the full-model regression were plotted against normal probability ranks to identify significant effects. A second regression was run with a reduced model including only the significant effects.

The half-normal probability plot of effects in Figure 11 shows that the temperature, dwell, temperature-dwell interaction, and dwell-adhesive interaction effects were significant for peak peel force. Figure 12 shows that the temperature, dwell, and temperature-pressure interaction were significant for average peel force. The main adhesive effect was not significant for either peak or average peel force. Appendix A35 includes normal and half-normal probability plots of effects for the full models, as well as plots of residuals for the reduced models which include the significant effects only.

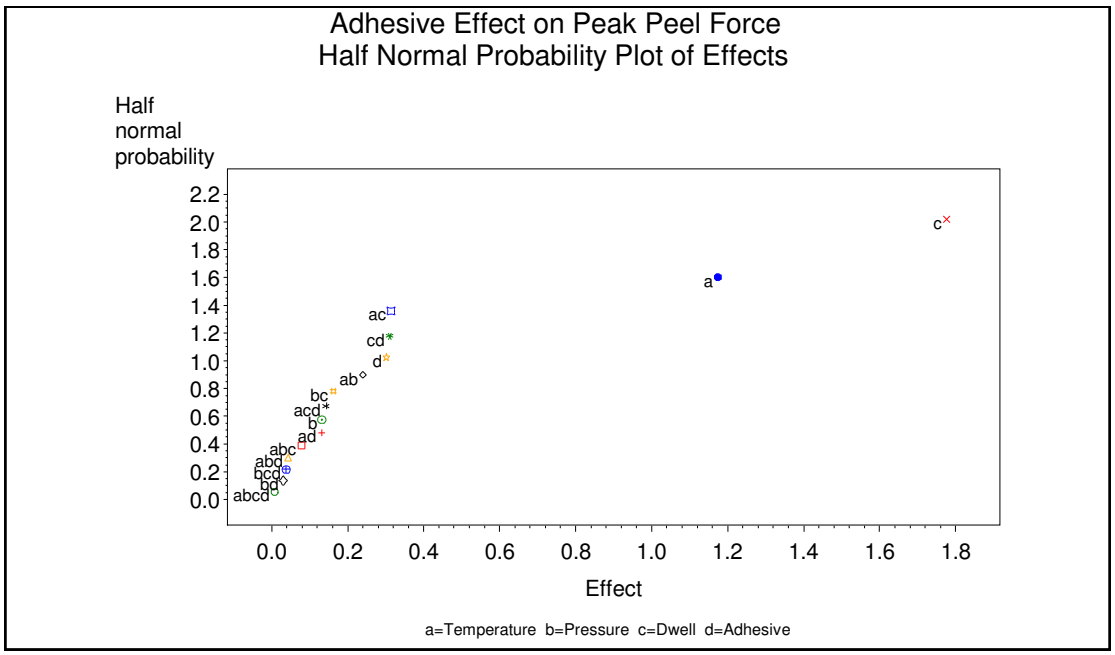

Figure 11. Half-normal probability plot of effects for peak peel force.

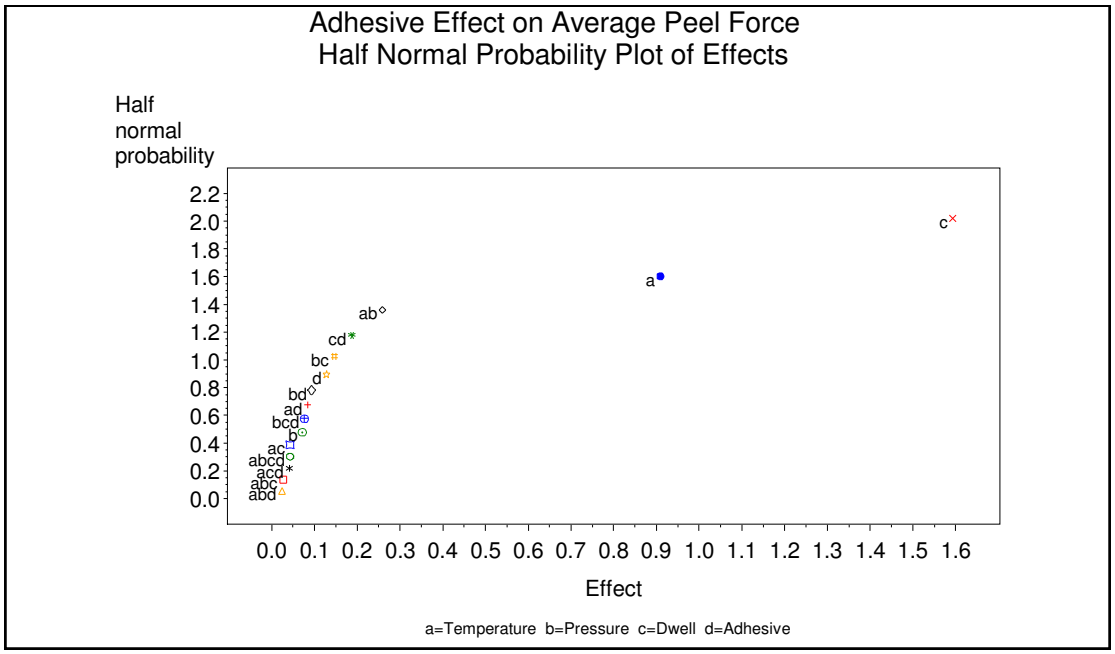

Figure 12. Half-normal probability plot of effects for average peel force.

Interpretation of results

The analysis clearly showed that tensile seal strength is not consistent around the package perimeter. The implication of this finding for industry is that the selection of locations for peel test specimens will impact the validity of the peel strength monitoring. If the specimens are taken from locations of higher peel strength, the conclusion that the seal meets it minimum tensile strength requirement may be invalid. Based on the analysis of the study specimens, the locations with the lowest peel strength will be close to the corners of the tray, so the areas around the corners should be sampled during peel testing.

The effects of process settings and specimen geometry on peel forces were depicted through box plots of peak and average force. Packages that were sealed on the same equipment had more consistent force values. However, some settings could be identified that produced relatively high peel forces and consistent variance for all packages except PS8. This indicates that it may be possible to develop standards for expected peel force based on process settings.

Category A, B, and C specimens tended to have higher peel forces than Category D and E specimens. Selection of specimen locations should consider the geometry of the specimen, since the selection of category A or B specimens may positively bias the estimate of minimum seal strength.

Average forces were less than peak forces, and tended to have less variability. Peak peel force may be more commonly used in industry since there is no calculation required, but peak peel force is not the preferred measure of minimum seal strength for practical as well as statistical reasons.

On a practical level, peel testing is intended to verify that the minimum seal strength specification of the package is met. The peak force, by definition, is higher than all other points in the specimen force profile, and the results of this research demonstrated that peak peel force was always higher than average peel force. Since peak peel force is the maximum force observed during the peel, it cannot represent the minimum seal strength of the specimen or of the package.

Statistically, the peak peel force provides a biased, highly variable estimate of the seal strength at the specimen location. The peel test of each specimen is basically a statistical experiment designed to estimate the strength of the tray at the specimen location. The sample size for the experiment equals the number of force-displacement data points recorded during the peel. Any valid statistical experiment must have a sample size greater than one. Deciding a priori that the estimate of seal strength of the specimen will equal the maximum force within the force profile essentially equates to using a sample size of one to estimate the seal strength and creates a biased estimate. There can be little confidence that this estimate represents the true value of the specimen seal strength. The peak peel force represents one instant in time on the force profile, and it does not seem rational to give this data point a weight of 100% to the exclusion of all other data points. In addition, the peak peel force measure has a higher variability than the average peel force measure. Consequently, the peak force may be significantly different from one tray to the next, meeting the specification on one tray and failing on the next. This will lead to continual adjustment of the sealing process parameters, introducing even more variation into the process.

Conversely, the average peel force provides a measure of minimum seal strength that is supportable practically and statistically. Statistically, the average peel force of the specimen is estimated based on a large sample size and makes use of all data obtained during peeling of the specimen. The average force provides an unbiased estimate of the seal strength of the specimen. Practically, the average peel force is always lower than the peak peel force, so it addresses the requirement to determine the minimum seal strength of the package for comparison to the minimum seal strength specification. Using the peak peel force as the estimate of the specimen seal strength can result in overestimation of the specimen seal strength. Comparing this overestimated strength to the minimum seal strength specification would lead to an erroneous conclusion that the minimum specification has been met. Processes that are certified as validated based on these overestimated seal strengths will produce packages whose true seal strengths fail to meet the predetermined specification. The results of this research indicated that peak force exceeded average force by a minimum of 4.64% and a maximum of 335%, and for 93% of specimens peak force was at least 10% higher than average force. This finding means that if peak peel force is being used for package design verification and sealing process validation, the estimate of seal strength may be overestimated by more than a factor of three.

There was not a significant difference in peel force between the two adhesives, although there was a significant interaction of adhesive with dwell time for the peak force response. Both adhesives were of the water-based flood-coated adhesive type, so it is reasonable that their performance results were generally comparable under the conditions tested. The overall assessment indicates that the two adhesives will produce very similar seal strengths, especially if average force is used as the measure.

CHAPTER IV

DEVELOPMENT OF EMPIRICAL MODELS OF PEEL FORCE FOR MEDICAL DEVICE TRAYS

Background

Tensile seal-strength (peel force) values of lidded trays are affected by characteristics of the packaging materials and by parameters of the package sealing process. In Chapter III an experiment was designed and carried out to collect data for the analysis of the effect of sealing process settings on peel force, using nine representative package configurations. In this chapter empirical models were developed to predict peel force as a function of seal process parameters, based on the data collected in Chapter III.

Model development

Method

Multiple linear regression analysis was used to fit models of peel force to the data from the peel force experiment presented in Chapter III (1131 specimens).

Regression was performed for two different peel force response variables: (1)peak peel force of the specimen that had the lowest peak peel force within a tray, and (2)average peel force of the specimen that had the lowest average peel force within a tray.

The regressors for the analyses were seal temperature, seal pressure and dwell time, entered into the models in all possible subsets. Each of these seven subset regressions was run with and without an intercept term, resulting in 14 models to be evaluated for each peel force response, and a total of 28 regression models fit.

The 14 regression models were fit for each response variable using three different groupings of the available study data. One grouping was by adhesive and package. There were nine package configurations in the study, one of which was sealed using both adhesives. The other eight packages were sealed using only one adhesive. Therefore, there were ten adhesive-package subsamples. Within each

subsample the 14 models were fit and compared for each peel force response, and model diagnostics were generated to identify the best models for the subsample.

Another grouping was according to similarities in tray material and shared sealing equipment. This grouping was intended to eliminate unexplained variation that may be due to differences in the tray material or the installation, maintenance, and operation of different sealing equipment. The two groupings were [PS1, PS2, PS4, PS7] and [PS3, PS6]. Within each package group the 14 models were fit and compared for each peel force response, and model diagnostics were generated to identify the best models for the group.

Finally, the regressions were run using all available samples ungrouped (N=1131 specimens). This overall dataset comprises packages of nine different sizes—some with slightly different tray materials—sealed with two different adhesives on five different sealers with various settings of seal temperature, seal pressure, and dwell time. The 14 models were fit and compared for each peel force response, and model diagnostics were generated to identify the best models for the sample. The variation in the study samples makes them representative of many of the package configurations in use; therefore the resulting model should have broad applicability.

All possible subsets models including SealTemp, SealPressure, and DwellTime were fit using SAS® Proc Reg with the RSQUARE selection criterion. The full model is shown in Equation 4.1.

$$\begin{aligned} \text{PeelForce} = {} & \beta_0 + \beta_1 \text{SealTemp} + \beta_2 \text{SealPressure} + \beta_{12} \text{SealTemp*SealPressure} \\ & + \beta_3 \text{DwellTime} + \beta_{13} \text{SealTemp*DwellTime} + \beta_{23} \text{SealPressure*DwellTime} \\ & + \beta_{123} \text{SealTemp*SealPressure*DwellTime} + \varepsilon \end{aligned} \tag{4.1}$$

The PeelForce term took on each of the two peel force responses described above. For ease of reference, each model configuration was given a name, as shown in Table 8. Each model was fit with β_0 estimated, and with β_0 assumed equal to zero (no intercept model).

Table 8. Model configurations for regression of peel force on sealing parameters

Model Name	Response Variable	Independent Variables			Grouping
PM1	PeakForce	SealTemp	SealPressure	DwellTime	Adhesive-Package
PM2	AvgForce	SealTemp	SealPressure	DwellTime	Adhesive-Package
PM3	PeakForce	SealTemp	SealPressure	DwellTime	Overall
PM4	AvgForce	SealTemp	SealPressure	DwellTime	Overall
PM5	PeakForce	SealTemp	SealPressure	DwellTime	Package group
PM6	AvgForce	SealTemp	SealPressure	DwellTime	Package group

For each model, R^2, adjusted R^2, Mallow's Cp, Akaike's Information Criterion (AIC), prediction error sum of squares (PRESS), and prediction R^2 statistics were calculated.

Akaike's Information Criterion (AIC) is a measure of goodness of fit that measures the difference between a given model and the true underlying model. The AIC includes a goodness of fit term derived from the log-likelihood of the model based on the sample data. The goodness of fit term decreases with each variable added. AIC also includes a penalty term which increases with each variable added. The AIC identifies the model within a predefined set of models that has the best fit to the given data using the fewest number of parameters; a lower value of AIC indicates a better model. When computed from least squares regression analyses, AIC is computed as

$$AIC = n \ln(SSE/n) + 2p \tag{4.2}$$

where SSE is the regression error sum of squares, p is the number of estimated parameters included in the model, and n is the number of observations.

For sample sizes resulting in $n/p < 40$, the corrected AIC is computed as

$$AIC_c = n \ln(SSE/n) + 2p + 2p(p+1)/(n-p-1) \tag{4.3}$$

The adjusted R^2 statistic is a modification of the R^2 statistic to account for the number of terms in the model. The regular R^2 statistic always increases when a new variable is added to the model, regardless of whether the additional variable is statistically significant or not, so a model with a high R^2 may not necessarily be a good model. The adjusted R^2 does not always increase when a new term is added, and may decrease if an unnecessary term is added. A large difference between the regular R^2 value and the adjusted R^2 value is an indication that nonsignificant terms may have been added to the model. The equation for adjusted R^2 is

$$R^2_{adj} = 1 - ((n-i)SSE / (n-p)SST) \quad (4.4)$$

where SSE is the regression error sum of squares, SST is the regression total sum of squares, p is the number of estimated parameters included in the model, n is the number of observations, and i=1 if there is an intercept in the model and i=0 otherwise.

The PRESS statistic is a scaled residual statistic that is used to measure the prediction error within a model. PRESS is calculated by summing the PRESS residuals of each observation in the sample, which are individually computed by fitting the regression without the selected observation and attempting to predict the observation's value using the remaining observations. PRESS should be low, and close to the mean squared error, for a good model. The prediction R^2 gives an indication of the predictive capability of the model, and is calculated from the PRESS statistic as

$$R^2_{pred} = 1- PRESS/SST \quad (4.5)$$

where SST is the regression total sum of squares.

Mallows C_p is a measure of the total squared error of the regression, defined as

$$C_p = SSE_p / s^2 + 2p - n \quad (4.6)$$

where s^2 is estimated by the mean squared error for the full model, SSE_p is the error sum of squares for a model with p parameters, and n is the number of observations. When the right model is selected, the parameter estimates are unbiased, and C_p will be close to p. A C_p value above p indicates that the parameter estimates are biased.

Within each subsample or group, the models were ranked by AIC, with lower AIC scores indicating better quality models. The model that was ranked number one by AIC was considered the best model within the group, unless the model had a negative adjusted R^2 or prediction R^2. In this case, the highest ranking model with positive R^2 statistics was considered the best model.

Results

Several regression analyses were completed separately for adhesive-package groups, package groups, and the overall sample. Externally studentized residuals were plotted against the regressors and predicted responses. There were no obvious patterns in these plots that would indicate severe changes in variance as the regressor or predicted response variables change. Normal probability plots of the residuals indicated that the errors were approximately normally distributed.

The models that ranked within the top five within each group according to AIC are summarized in Appendices A12, A13, and A14. Each summary includes a table with model parameter estimates, fit statistics, and model diagnostics and a table with ANOVA statistics for the regression.

Analysis by adhesive and package

Appendix A12 includes a summary of the regression analyses by Adhesive and Package. A review of these data reveals that the top five ranking models all had favorable results for the Cp, PRESS, and RMSE model diagnostics. Cp was equal to p, which indicates a lack of bias. PRESS was very close to SSE, and RMSE was low. R^2 and adjusted R^2 were close, so no overfitting was indicated.

The five models differed most in R^2 values. Models that included the intercept term had significantly lower R^2 values than the models fit through the origin. All of the models that were highest ranked by AIC included the intercept term. In each model that included the intercept term, the intercept was significant at p-value <= .05, with one exception. In the average force models fit to package PS9 data, the intercept term had a p-value =.07; Seal Temperature was the only significant term in these models.

It is plausible that regression through the origin (RTO) would be applicable to the response variables studied, since the seal strength would be expected to equal zero if the temperature, pressure, and dwell time are zero. Nevertheless, the models with intercept terms achieved lower AIC scores. As a check whether RTO might be appropriate, the peak and average forces were plotted against three parameter levels: 'Low' = SealTemp 240/SealPressure 75/DwellTime 3, 'Med' = SealTemp 260/SealPressure 85/DwellTime 4.5, and 'High" = SealTemp 290/SealPressure 95/DwellTime 6.5. These plots are included in Appendix A21, and indicate that the peel forces are approximately linear in the parameter levels. For some of the packages the line of best fit appears to pass through the origin, so it is possible that the RTO models may provide acceptable results in application.

Seal Temperature was significant in all peak force and average force models. Dwell Time was significant in all models with the exception of the PS9 models for average force. Dwell Time was a more important parameter than temperature, with coefficients in the range of seven to 40 times the coefficients of temperature. Seal Pressure was not significant in most of the models; it was significant in all models for PS5 and PS6, the 5th ranked model for PS3, the first four peak force models for PS7, and most of the PS8 models.

Table 9 summarizes the coefficients and adjusted R^2 values among the 1st ranked models. The coefficients for Seal Temperature were very consistent across the packages, as shown in Table 9. Seal Pressure coefficients were slightly less consistent, while there was considerably more variation in the Dwell Time coefficients. The intercepts also varied significantly across the packages. Adjusted R^2 values were below 70% for most of the packages, although two had adjusted and prediction R^2 values of around 80% for average force.

Table 9. Summary of parameters for adhesive-package peel force regression models with lowest AIC score

Dependent Variable	Parameter	Minimum Value	Maximum Value	Range
Peak Force	Intercept	-14.42	-5.13	9.29
	Seal Temperature	.04	.05	.01
	Seal Pressure	-.02	.03	.05
	Dwell Time	0	1.17	1.17
	Adjusted R^2	.26	.69	.43
	Prediction R^2	.22	.68	.46
Average Force	Intercept	-13.14	-2.30	10.84
	Seal Temperature	.03	.05	.02
	Seal Pressure	-.02	.02	.04
	Dwell Time	0	1.00	1.00
	Adjusted R^2	.18	.80	.62
	Prediction R^2	.15	.80	.65

Table 10 summarizes the coefficients and adjusted R^2 values for the highest ranking models with an adjusted $R^2 > .79$.

Table 10. Summary of parameters for adhesive-package peel force regression models with lowest AIC score and adjusted $R^2 > .79$

Dependent Variable	Parameter	Minimum Value	Maximum Value	Range
Peak Force	Intercept	0	0	0
	Seal Temperature	.01	.03	.02
	Seal Pressure	-.07	0	.07
	Dwell Time	0	1.06	1.06
	Adjusted R^2	.91	.99	.08
	Prediction R^2	.91	.99	.08
Average Force	Intercept	0	0	0
	Seal Temperature	.01	.04	.03
	Seal Pressure	-.04	0	.04
	Dwell Time	0	1.00	1.00
	Adjusted R^2	.93	.99	.06
	Prediction R^2	.93	.99	.06

The models selected for each package based on high R^2 have adjusted R^2 values of .91 to .99. These models include Seal Temperature, Seal Pressure and Dwell Time only, with the intercept forced to zero. The difference in the AIC scores between the 1st ranked model and the no-intercept model ranges from .72 to 82.27.

Tables 11 and 12 list the details for the highest ranking models based on AIC score and the highest ranking models with an adjusted R^2 greater than .79.

Table 11. Best models for peak force by adhesive and package

Dependent Variable	Adhesive	Package	Model	Model ID	Intercept	Seal Temp	Seal Pressure	Dwell Time	Adjusted R^2	Prediction R^2	N	AIC	MSE	AIC rank	Selected by	AIC Difference
PeakForce	Amcor	PS1	PM1	PM1-1	-9.50	0.05	.	0.39	0.47	0.44	96	-58.83	0.53	1	A	
		PS1	PM1	PM1-3	.	0.01	.	0.33	0.98	0.98	96	-38.53	0.66	3	R	20.3
		PS2	PM1	PM1-1	-7.98	0.05	.	0.39	0.58	0.56	96	-113.94	0.30	1	A	
		PS2	PM1	PM1-3	.	0.01	.	0.34	0.99	0.99	96	-88.70	0.39	3	R	25.24
		PS3	PM1	PM1-1	-13.46	0.05	0.02	0.47	0.62	0.61	119	-0.51	0.96	1	A	
		PS3	PM1	PM1-5	.	0.03	-0.04	0.36	0.94	0.94	119	53.97	1.54	5	R	54.48
		PS4	PM1	PM1-1	-5.17	0.04	.	0.37	0.39	0.36	84	-54.44	0.51	1	A	
		PS4	PM1	PM1-3	.	0.02	.	0.34	0.98	0.98	84	-49.90	0.54	3	R	4.54
		PS5	PM1	PM1-1	-13.09	0.05	0.02	0.33	0.63	0.62	136	-30.66	0.78	1	A	
		PS5	PM1	PM1-5	.	0.03	-0.03	0.22	0.95	0.95	136	40.38	1.32	5	R	71.04
		PS6	PM1	PM1-1	-9.54	0.04	0.02	0.50	0.63	0.62	136	-58.27	0.63	1	A	
		PS6	PM1	PM1-3	.	0.02	-0.02	0.43	0.97	0.97	136	-8.50	0.92	3	R	49.77
		PS7	PM1	PM1-1	-10.33	0.05	0.03	0.23	0.26	0.22	96	1.62	0.98	1	A	
		PS7	PM1	PM1-5	.	0.02	.	0.18	0.97	0.97	96	10.33	1.09	5	R	8.71
		PS8	PM1	PM1-1	-9.29	0.04	-0.02	0.81	0.67	0.66	136	-11.84	0.89	1	A	
		PS8	PM1	PM1-3	.	0.02	-0.06	0.74	0.93	0.93	136	23.07	1.16	3	R	34.91
		PS9	PM1	PM1-1	-5.13	0.04	0.01	0.08	0.39	0.36	96	-140.77	0.22	1	A	
		PS9	PM1	PM1-5	.	0.02	.	.	0.99	0.99	96	-131.53	0.25	5	R	9.24
	Perfecseal	PS8	PM1	PM1-1	-14.42	0.05	.	1.17	0.69	0.68	136	63.31	1.56	1	A	
		PS8	PM1	PM1-3	.	0.02	-0.07	1.06	0.91	0.91	136	106.46	2.14	3	R	43.15

Table 12. Best models for average force by adhesive and package

Dependent Variable	Adhesive	Package	Model	Model ID	Intercept	Seal Temp	Seal Pressure	Dwell Time	Adjusted R^2	Prediction R^2	N	AIC	MSE	AIC rank	Selected by	AIC Difference
AvgForce	Amcor	PS1	PM2	PM2-1	-8.82	0.05	.	0.35	0.47	0.44	96	-82.69	0.41	1	A	
		PS1	PM2	PM2-3	.	0.01	.	0.29	0.97	0.97	96	-60.31	0.52	3	R	22.38
		PS2	PM2	PM2-1	-9.74	0.04	0.01	0.42	0.60	0.58	96	-115.03	0.29	1	A	
		PS2	PM2	PM2-3	.	0.01	.	0.37	0.98	0.98	96	-85.05	0.40	3	R	29.98
		PS3	PM2	PM2-1	-13.14	0.05	0.02	0.51	0.68	0.67	119	-36.96	0.71	1	A	
		PS3	PM2	PM2-5	.	0.02	-0.04	0.41	0.93	0.93	119	30.14	1.26	5	R	67.10
		PS4	PM2	PM2-1	-4.36	0.03	.	0.32	0.29	0.26	84	-47.75	0.55	1	A	
		PS4	PM2	PM2-3	.	0.01	.	0.30	0.97	0.97	84	-45.39	0.57	3	R	2.36
		PS5	PM2	PM2-1	-11.34	0.04	0.02	0.34	0.67	0.66	136	-95.34	0.48	1	A	
		PS5	PM2	PM2-5	.	0.02	-0.03	0.25	0.95	0.95	136	-13.07	0.89	5	R	82.27
		PS6	PM2	PM2-1	-10.25	0.04	0.02	0.54	0.67	0.65	136	-72.81	0.57	1	A	
		PS6	PM2	PM2-3	.	0.02	-0.03	0.46	0.95	0.95	136	-11.33	0.90	3	R	61.48
		PS7	PM2	PM2-1	-7.37	0.05	.	0.22	0.18	0.15	96	9.02	1.07	1	A	
		PS7	PM2	PM2-4	.	0.02	.	0.17	0.96	0.96	96	14.20	1.14	4	R	5.18
		PS8	PM2	PM2-1	-8.07	0.03	-0.02	0.79	0.80	0.79	136	-124.29	0.39	1	A and R	N/A
		PS9	PM2	PM2-1	-2.30	0.03	.	.	0.20	0.18	96	-117.21	0.29	1	A	
		PS9	PM2	PM2-2	.	0.02	.	.	0.99	0.99	96	-116.49	0.29	2	R	.72
	Perfecseal	PS8	PM2	PM2-1	-12.02	0.04	.	1.00	0.80	0.80	136	-67.50	0.60	1	A and R	N/A

Analysis by package group

Appendix A13 includes a summary of the regression analyses by package groups. A review of these data reveals that the top five ranking models all had favorable results for the Cp, PRESS, and RMSE model diagnostics. Cp was equal to p, which indicates a lack of bias. PRESS was very close to SSE, and RMSE was low. R^2 and adjusted R^2 were close, so no overfitting was indicated.

The five models differed most in R^2 values. Models that included the intercept term had significantly lower R^2 values than the models fit through the origin. All of the models that were highest ranked by AIC included the intercept term. In each model that included the intercept term, the intercept was significant at p-value <= .05.

Seal Temperature and Dwell Time were significant in all peak force and average force models. Seal Pressure was significant in all of the models except the 3rd and 4th ranked model for package group [PS1 PS2 PS4 PS7]. Dwell Time was a more important parameter than temperature and pressure, with coefficients in the range of seven to 40 times the coefficients of temperature and pressure.

Table 13 summarizes the coefficients and adjusted R^2 values among the 1st ranked models. The coefficients for Seal Temperature and Seal Pressure were very consistent between the package groups, as shown in Table 13. There was considerably more variation in the dwell time coefficients, just as observed with the adhesive-package regressions. The intercepts also varied significantly across the packages. Adjusted R^2 values were below 70% for both groups. The ranges of all of the parameter coefficients and R^2 values were lower for the package group analysis than for the adhesive-package analysis. The adjusted R^2 values for group [PS3 PS6] were equivalent to the R^2 values for the individual packages. By contrast, the adjusted R^2 values for group [PS1 PS2 PS4 PS7] were lower than the R^2 values for most of the individual packages.

Table 13. Summary of parameters for package group peel force regression models with lowest AIC score

Dependent Variable	Parameter	Minimum Value	Maximum Value	Range
Peak Force	Intercept	-11.37	-8.84	2.53
	Seal Temperature	.05	.05	0
	Seal Pressure	.01	.02	.01
	Dwell Time	.34	.49	.15
	Adjusted R^2	.34	.61	.27
	Prediction R^2	.34	.61	.27
Average Force	Intercept	-11.60	-8.42	3.18
	Seal Temperature	.04	.04	0
	Seal Pressure	.01	.02	.01
	Dwell Time	.33	.53	.20
	Adjusted R^2	.32	.67	.35
	Prediction R^2	.31	.66	.35

Table 14 summarizes the coefficients and adjusted R^2 values for the highest ranking models that also have adjusted $R^2 > .79$.

Table 14. Summary of parameters for package group peel force regression models with lowest AIC score and adjusted $R^2 > .79$

Dependent Variable	Parameter	Minimum Value	Maximum Value	Range
Peak Force	Intercept	0	0	0
	Seal Temperature	.02	.02	0
	Seal Pressure	-.03	0	.03
	Dwell Time	.30	.40	.10
	Adjusted R^2	.95	.97	.02
	Prediction R^2	.95	.97	.02
Average Force	Intercept	0	0	0
	Seal Temperature	.01	.02	.01
	Seal Pressure	-.04	0	.04
	Dwell Time	.28	.44	.16
	Adjusted R^2	.94	.97	.03
	Prediction R^2	.94	.97	.03

The peak force model selected for group [PS1 PS2 PS4 PS7] based on high R^2 has an adjusted R^2 of .97. The average force model selected for group [PS1 PS2 PS4 PS7] based on high R^2 has an adjusted R^2 of .97. These models include Seal Temperature, Seal Pressure and Dwell Time only, with the intercept forced to zero. The difference in the AIC scores for the two peak force models is 43.31. The difference in the AIC scores for the two average force models is 42.42.

The peak force model selected for group [PS3 PS6] based on high R^2 has an adjusted R^2 of .95. The average force model selected for group [PS3 PS6] based on high R^2 has an adjusted R^2 of .94. These models include Seal Temperature, Seal Pressure and Dwell Time only, with the intercept forced to zero. The difference in the AIC scores for the two peak force models is 103.26. The difference in the AIC scores for the two average force models is 128.38.

Table 15 lists the details for the highest ranking models based on AIC score and the highest ranking models with an adjusted R^2 greater than .79.

Table 15. Best models for peak and average force by package group

Dependent Variable	Package Group	Model	Model ID	Intercept	Seal Temp	Seal Pressure	Dwell Time	Adjusted R^2	Prediction R^2	N	AIC	MSE	AIC rank	Selected by
PeakForce	PS1 PS2 PS4 PS7	PM5	PM5-1	-8.84	0.05	0.01	0.34	0.34	0.34	372	-117.88	0.72	1	A
		PM5	PM5-3	.	0.02	.	0.30	0.97	0.97	372	-74.57	0.81	3	R
	PS3 PS6	PM5	PM5-1	-11.37	0.05	0.02	0.49	0.61	0.61	255	-52.08	0.80	1	A
		PM5	PM5-3	.	0.02	-0.03	0.40	0.95	0.95	255	51.18	1.21	3	R
AvgForce	PS1 PS2 PS4 PS7	PM6	PM6-1	-8.42	0.04	0.01	0.33	0.32	0.31	372	-146.04	0.67	1	A
		PM6	PM6-3	.	0.01	.	0.28	0.97	0.97	372	-103.62	0.75	3	R
	PS3 PS6	PM6	PM6-1	-11.60	0.04	0.02	0.53	0.67	0.66	255	-109.89	0.64	1	A
		PM6	PM6-3	.	0.02	-0.04	0.44	0.94	0.94	255	18.49	1.06	3	R

Analysis over all packages

Appendix A14 includes a summary of the regression analyses over all packages. A review of these data reveals that the top five ranking models all had favorable results for the Cp, PRESS, and RMSE model diagnostics. Cp was equal to p, which indicates a lack of bias. PRESS was very close to SSE, and RMSE was low. R^2 and adjusted R^2 were close, so no overfitting was indicated.

The five models differed most in R^2 values. Models that included the intercept term had significantly lower R^2 values than the models fit through the origin. The model that was highest ranked by AIC included the intercept term. In each model that included the intercept term, the intercept was significant at p-value <= .05.

Seal Temperature and Dwell Time were significant in all peak force and average force models. Seal Pressure was not significant in most of the models; it was significant in the 3rd and 4th ranked model for package group [PS1 PS2 PS4 PS7]. Dwell Time was a more important parameter than temperature and pressure, with coefficients in the range of seven to 40 times the coefficients of temperature and pressure.

Table 16 summarizes the coefficients and adjusted R^2 values for the 1st ranked models. The adjusted R^2 values were below 70% for peak and average force.

Table 16. Summary of parameters for overall peel force regression models with lowest AIC score

Dependent Variable	Parameter	Value
Peak Force	Intercept	-6.76
	Seal Temperature	.03
	Seal Pressure	.01
	Dwell Time	.52
	Adjusted R^2	.32
	Prediction R^2	.32
Average Force	Intercept	-6.01
	Seal Temperature	.03
	Seal Pressure	.01
	Dwell Time	.50
	Adjusted R^2	.31
	Prediction R^2	.31

Table 17 summarizes the coefficients and adjusted R^2 values for the highest ranking models that also have adjusted $R^2 > .79$.

Table 17. Summary of parameters for overall peel force regression models with lowest AIC score and adjusted $R^2 > .79$

Dependent Variable	Parameter	Value
Peak Force	Intercept	0
	Seal Temperature	.02
	Seal Pressure	-.02
	Dwell Time	.47
	Adjusted R^2	.94
	Prediction R^2	.94
Average Force	Intercept	0
	Seal Temperature	.01
	Seal Pressure	-.02
	Dwell Time	.45
	Adjusted R^2	.92
	Prediction R^2	.92

The peak force model selected based on high R^2 has an adjusted R^2 of .94. The average force model selected based on high R^2 has an adjusted R^2 of .92. These models include Seal Temperature, Seal Pressure and Dwell Time only, with the intercept forced to zero. The difference in the AIC scores for the two peak force models is 80.45. The difference in the AIC scores for the two average force models is 74.30.

Table 18 lists details for the highest ranking models based on AIC score and the highest ranking models with an adjusted R^2 greater than .79.

Table 18. Best models for peak and average force over all packages

Dependent Variable	Model	Model ID	Intercept	Seal Temp	Seal Pressure	Dwell Time	Adjusted R^2	Prediction R^2	N	AIC	MSE	AIC rank	Sel by
PeakForce	PM3	PM3-1	-6.76	0.03	0.01	0.52	0.32	0.32	1131	546.95	1.62	1	A
	PM3	PM3-3	.	0.02	-0.02	0.47	0.94	0.94	1131	627.40	1.74	3	R
AvgForce	PM4	PM4-1	-6.01	0.03	0.01	0.50	0.31	0.31	1131	372.73	1.39	1	A
	PM4	PM4-3	.	0.01	-0.02	0.45	0.92	0.92	1131	447.03	1.48	3	R

Interpretation of results

Over the range of seal pressure values studied, seal pressure was not as important as dwell time and temperature for predicting peel strength. Similarly, over the range of temperatures studied, the importance of temperature was evident, but not as strongly as the importance of dwell time. Since dwell time had very large coefficients compared to temperature, small changes in dwell time would be expected to cause significant changes in peel strength.

Adjusted R^2 values were very low for most of the models fit without forcing the line through the origin. However, with regression through the origin, very high R^2 values resulted. Some of the RTO regressions resulted in AIC scores that were higher by 128 points, but the majority of differences were less than 60 points. The RTO models would be applicable if it is believed that the response should be zero if the three parameters are zero, and that the linear relationship is continuous from the study range to the origin. The plots presented in Appendix A21 support the possibility that RTO models may provide acceptable results in application, but this needs to be confirmed by further investigation.

The variability in the coefficients of the intercept and dwell time parameters for the adhesive-package and package group analyses reduce the usefulness of those models for the development of general prediction equations. In contrast, the selected models developed from the overall analysis should be generally applicable and had high adjusted and prediction R^2 values. The predictive equations based on these overall RTO models are given in Table 19. The lower coefficients for average force agree with the descriptive statistics and graphical analyses that showed that average peel force is lower than peak peel force.

Table 19. Predictive equations for peel force based on sealing parameters

Equation	Adjusted R^2	Prediction R^2
Peak Force = 0.02*Seal Temperature – 0.02*Seal Pressure + 0.47*DwellTime	.94	.94
Average Force = 0.01*Seal Temperature – 0.02*Seal Pressure + 0.45*DwellTime	.92	.92

CHAPTER V

EFFECT OF MEDICAL DEVICE TRAY CHARACTERISTICS AND PACKAGING PROCESS PARAMETERS ON BURST PRESSURE

Experiment

Statement of the problem

Inflation seal-strength (burst pressure) values of lidded trays are affected by characteristics of the packaging materials and by parameters of the package sealing and burst testing processes. This experiment investigated the effects of sealing temperature, sealing pressure, dwell time, tray length-to-width ratio, lid area, and restraining plate gap distance on burst pressure, as well as the difference in effects of two different sealing adhesives.

Response

The response studied in this experiment was burst pressure, the internal package pressure required to separate the seal, measured in pouds per square inch (psi).

Factors

The factors investigated were sealing pressure, dwell time, sealing temperature, tray length-to-width ratio, lid area, restraining plate gap distance, and adhesive. The factors controlled were tray material and lid material. Variables that were measured but not controlled were seal width (in.), tray volume (fl oz), and tray height (in.).

Research and discussions with medical device packaging industry leaders identified the range of several package characteristics that would encompass a wide range of medical device packages that are in use and expected to be in use during the next five years. Packages were sought and selected into the study to reflect these characteristics, in order to give the developed model broader applicability. Specifically, PETG was selected as the tray material, as it is used predominately by manufacturers of high-end medical devices. For the same reason, the lid stock selected was Tyvek 1073B. The two water-based adhesives selected are the most popular for their respective manufacturers.

Nine trays of various areas, volumes and length-to-width ratios were sealed with 27 different combinations of seal pressure, seal temperature, and dwell time. Trays were selected to yield three levels of area and three levels of length-to-width ratio. The minimum and maximum seal process settings were selected to cover the range of values for these settings that are likely to be used in the industry.

A restrained burst test was selected because when a package is unrestrained, some of the internal force is directed toward expanding the lid, rather than being distributed directly onto the seal area. Since terminally sterilized medical devices are sterilized and shipped inside boxes, the lid is not free to expand in an unrestrained manner. Therefore, the unrestrained burst test does not create a true simulation of the forces that will be exerted on the seal in real application. Three levels of gap distance were selected to cover a wide range of possible clearances of the lid when the tray is inside its box.

Factor descriptions and types, number of levels, units of measure, and effect types are given in Table 20.

Materials

Nine tray configurations were used in the experiment, as described in Table 2, presented in Chapter III. The trays were sealed with Tyvek 1073B lids coated with Amcor 2635B or Perfecseal CR-27 adhesive.

Table 20. Burst pressure experiment factors

Factor	Description	UOM	Factor Type	Levels	Effect Type
SealPressure	Pressure applied to join lid to tray	psi	Quantitative	75 / 85 / 95	Random
DwellTime	Amount of time pressure is applied at a temperature high enough to activate the adhesive	sec	Quantitative	3 / 4.5 / 6.5	Random
SealTemp	Temperature applied to join lid to tray	F	Quantitative	240 / 260 / 290	Random
Adhesive	Bonding agent applied to lid	N/A	Qualitative	2635B / CR-27	Fixed
LenWidth	Tray length-to-width ratio	N/A	Quantitative	< 1.7 (Low) 1.7-3.6 (Med) > 3.6 (High)	Random
TrayArea	Area of tray within the seal perimeter	sq in.	Quantitative	< 60 (Low) 60-83 (Med) > 83 (High)	Random
Gap	Distance from top of lid to restraining plate	in.	Quantitative	.25 / .50 / .75	Random
TrayMaterial	Plastic from which tray is formed	N/A	Qualitative	PETG	Fixed
LidMaterial	Lid stock from which lid is cut	N/A	Qualitative	Tyvek 1073B	Fixed

Methods

Packages were heat sealed and then inspected according to the F1886-98 standard for visual inspection of medical package seals. [8] The locations of all voids, overheated areas and flange deformation were recorded using code 1 for voids, code 2 for overheating, and code 3 for flange deformation.

The sealed packages were burst tested according to the F2054-00 burst testing standard for restrained burst testing.[10] The sealing equipment, burst test equipment, and experimental conditions for each package are given in Table 21. Figure 13 shows the burst test equipment with a tray in position to be tested. The burst pressure and burst location of each package were recorded.

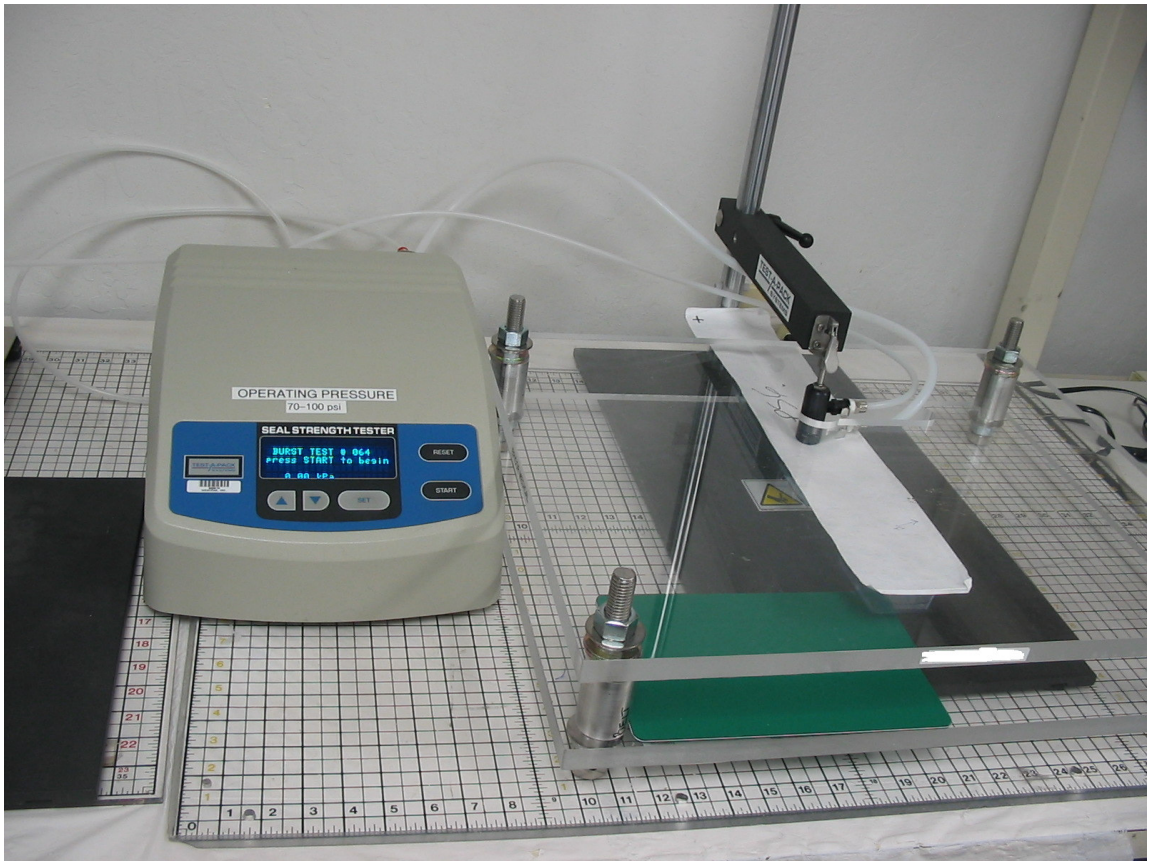

Figure 13. Burst test equipment with tray loaded.

Design

Design selection

To study the burst pressure response to SealTemp, SealPressure, DwellTime, LenWidth, TrayArea, and Gap a Resolution-V fractional factorial with 27 runs as defined in Table 22 was used.

To study the burst pressure response to Adhesive, the 27 runs of the fractional factorial were run at the two levels of Adhesive with one package configuration (PS8).

Table 21. Burst pressure experimental conditions

Package	Sealer	Room Temp (C)	RH %	Burst Tester	Flow Rate	Sensitivity	Prefill	Room Temp (C)	RH %
PS1	Alloyd 2S1428 #02	22	50	ARO F100-2500-1	5	1	Y	22	50
PS2	Alloyd 2S1428 #02	22	50	ARO F100-2500-1	5	1	Y	22	50
PS3	Alloyd 2S1428 #03	22	50	ARO F100-2500-1	5	1	Y	22	50
PS4	Alloyd 2S1428 #02	22	50	ARO F100-2500-1	5	1	Y	22	50
PS5	Alloyd 2SM1428 #01	22	50	ARO F100-2500-1	5	1	Y	22	50
PS6	Alloyd 2S1428 #03	22	50	ARO F100-2500-1	5	1	Y	22	50
PS7	Alloyd 2S1428 #02	22	50	ARO F100-2500-1	5	1	Y	22	50
PS8	Alloyd 2SM1428 #04	21	48	Test-A-Pack F100-2600-3	5	1	Y	23	50
PS9	Belco BM2020 #05	22	50	ARO F100-2500-1	5	1	Y	22	50

Replication

Nine replicates of the experiment were run, with Adhesive varied in replicate one only. In replicates two through eight, Adhesive was fixed at 2635B only.

Data from all nine replicates were analyzed to investigate the effect of SealTemp, SealPressure, DwellTime, LenWidth, TrayArea, and Gap. The sample size for this data set was 243 (9 replicates x 27 runs).

Data from replicate one were analyzed to investigate the effect of Adhesive. The sample size for this data set was 54 (1 replicate x 54 runs).

Table 22. Burst pressure fractional factorial design runs

SealTemp	SealPressure	DwellTime	Gap	Seal Setting
240	75	3	0.25	S1
240	75	4.5	0.75	S2
240	75	6.5	0.5	S3
240	85	3	0.75	S4
240	85	4.5	0.5	S5
240	85	6.5	0.25	S6
240	95	3	0.5	S7
240	95	4.5	0.25	S8
240	95	6.5	0.75	S9
260	75	3	0.75	S10
260	75	4.5	0.5	S11
260	75	6.5	0.25	S12
260	85	3	0.5	S13
260	85	4.5	0.25	S14
260	85	6.5	0.75	S15
260	95	3	0.25	S16
260	95	4.5	0.75	S17
260	95	6.5	0.5	S18
290	75	3	0.5	S19
290	75	4.5	0.25	S20
290	75	6.5	0.75	S21
290	85	3	0.25	S22
290	85	4.5	0.75	S23
290	85	6.5	0.5	S24
290	95	3	0.75	S25
290	95	4.5	0.5	S26
290	95	6.5	0.25	S27

Randomization

After each change in seal temperature, the sealing equipment had to stabilize for at least 20 minutes. Sealer pressure also had to be stabilized after each change by cycling the sealer platen two or three times and readjusting the pressure control valve until the desired pressure was set and stable. Due to the length of time required to change seal temperature and seal pressure, runs were not completely randomized. A split-split-plot design, illustrated in Figure 14, was used to complete the runs, with temperature in the whole plot, pressure in the subplot, and dwell time, adhesive, and gap randomized within the subplot. The order of the whole plots was random, as was the order of the subplots within each whole plot.

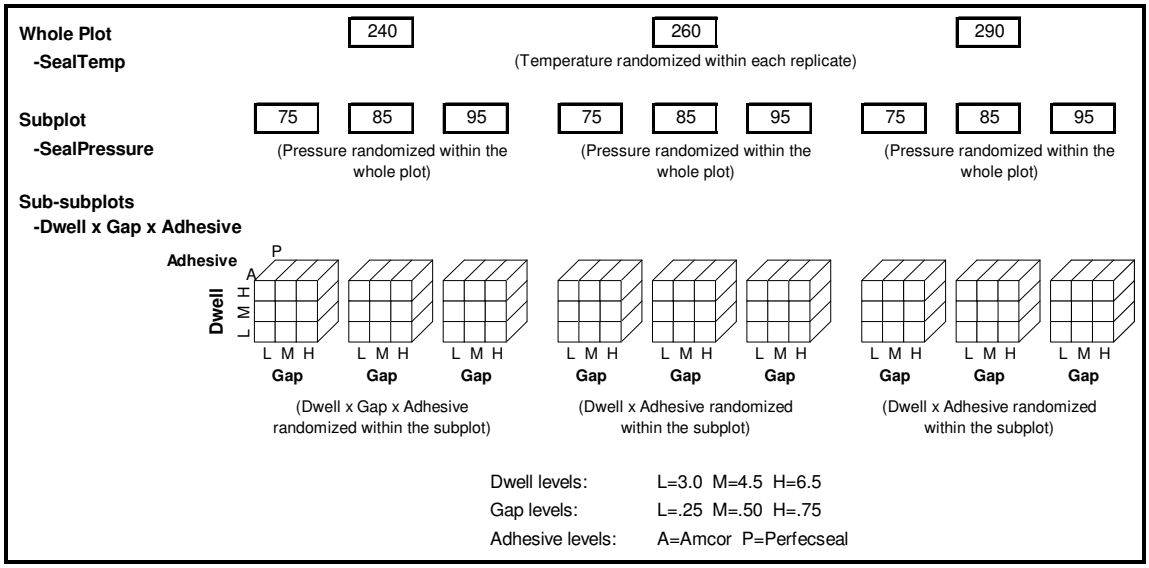

Figure 14. Split-split-plot design for burst pressure.

Blocking

The fractional factorial design was replicated for each of the nine package configurations. Due to potential effects of differences in package geometries, Package was treated as a blocking variable. Since each replicate sealed a different package, the effects of the package factors (LenWidth and TrayArea) are included in the effects of the replicates/blocks.

Statistical models

The linear statistical model for the split-split-plot design to study the effect of Adhesive is

$$
\begin{aligned}
y_{jklm} &= \mu + \beta_j + \gamma_k + (\beta\gamma)_{jk} + \delta_l + (\beta\delta)_{jl} + (\gamma\delta)_{kl} + (\beta\gamma\delta)_{jkl} + \lambda_m + (\beta\lambda)_{jm} + (\gamma\lambda)_{km} \\
&+ (\delta\lambda)_{lm} + (\beta\gamma\lambda)_{jkm} + (\beta\delta\lambda)_{jlm} + (\gamma\delta\lambda)_{klm} + (\beta\gamma\delta\lambda)_{jklm} + \rho_p + (\beta\rho)_{jp} + (\gamma\rho)_{kp} + (\delta\rho)_{lp} \\
&+ (\beta\gamma\rho)_{jkp} + (\beta\delta\rho)_{jdp} + (\gamma\delta\rho)_{kdp} + (\rho\lambda)_{pm} + (\beta\rho\lambda)_{jpm} + (\gamma\rho\lambda)_{kpm} + (\delta\rho\lambda)_{lpm} \\
&+ (\beta\gamma\delta\rho)_{jklp} + (\beta\gamma\rho\lambda)_{jkpm} + (\beta\delta\rho\lambda)_{jlpm} + (\gamma\delta\rho\lambda)_{klpm} + (\beta\gamma\delta\rho\lambda)_{jklpm} \\
&+ \varepsilon_{jklpm} \qquad \begin{cases} j = 1, 2, 3 & \text{(SealTemp)} \\ k = 1, 2, 3 & \text{(SealPressure)} \\ l = 1, 2, 3 & \text{(DwellTime)} \\ m = 1, 2 & \text{(Adhesive)} \\ p = 1, 2, 3 & \text{(Gap)} \end{cases}
\end{aligned}
\tag{5.1}
$$

where the effects in the model correspond to the study factors as listed in Table 23.

The linear statistical model for the split-split-plot design to study the effect of SealTemp, SealPressure, DwellTime, and Gap is

$$
\begin{aligned}
y_{ijklm} &= \mu + \tau_i + \beta_j + (\tau\beta)_{ij} + \gamma_k + (\tau\gamma)_{ik} + (\beta\gamma)_{jk} + (\tau\beta\gamma)_{ijk} + \delta_l + (\tau\delta)_{il} + (\beta\delta)_{jl} + (\tau\beta\delta)_{ijl} \\
&+ (\gamma\delta)_{kl} + (\tau\gamma\delta)_{ikl} + (\beta\gamma\delta)_{jkl} + (\tau\beta\gamma\delta)_{ijkl} + \rho_p + (\tau\rho)_{ip} + (\beta\rho)_{jp} + (\tau\beta\rho)_{ijp} + (\gamma\rho)_{kp} \\
&+ (\tau\gamma\rho)_{ikp} + (\delta\rho)_{lp} + (\tau\delta\rho)_{ilp} + (\beta\gamma\rho)_{jkp} + (\tau\beta\gamma\rho)_{ijkp} + (\beta\delta\rho)_{jdp} + (\tau\beta\delta\rho)_{ijdp} + (\gamma\delta\rho)_{kdp} + (\tau\gamma\delta\rho)_{ikdp} + \\
&(\beta\gamma\delta\rho)_{jklp} + (\tau\beta\gamma\delta\rho)_{ijklp} \\
&+ \varepsilon_{ijklp} \qquad \begin{cases} i = 1, 2, \ldots, 9 & \text{(Replicates)} \\ j = 1, 2, 3 & \text{(SealTemp)} \\ k = 1, 2, 3 & \text{(SealPressure)} \\ l = 1, 2, 3 & \text{(DwellTime)} \\ p = 1, 2, 3 & \text{(Gap)} \end{cases}
\end{aligned}
\tag{5.2}
$$

where the effects in the model correspond to the study factors as listed in Table 24.

Table 23. Factor effects for the split-split-plot design for studying effect of adhesive on burst pressure

Element	Factor	Effect
Whole plot	SealTemp main effect	β_j
Subplot	SealPressure main effect	γ_k
	SealTemp x SealPressure interaction (Subplot error)	$(\beta\gamma)_{jk}$
Sub-subplot	DwellTime main effect	δ_l
	SealTemp x DwellTime interaction	$(\beta\delta)_{jl}$
	SealPressure x DwellTime interaction	$(\gamma\delta)_{kl}$
	SealTemp x SealPressure x DwellTime interaction	$(\beta\gamma\delta)_{jkl}$
	Adhesive main effect	λ_m
	SealTemp x Adhesive interaction	$(\beta\lambda)_{jm}$
	SealPressure x Adhesive interaction	$(\gamma\lambda)_{km}$
	DwellTime x Adhesive interaction	$(\delta\lambda)_{lm}$
	SealTemp x SealPressure x Adhesive interaction	$(\beta\gamma\lambda)_{jkm}$
	SealTemp x DwellTime x Adhesive interaction	$(\beta\delta\lambda)_{jlm}$
	SealPressure x DwellTime x Adhesive interaction	$(\gamma\delta\lambda)_{klm}$
	SealTemp x SealPressure x DwellTime x Adhesive	$(\beta\gamma\delta\lambda)_{jklm}$
	Gap main effect	ρ_p
	SealTemp x Gap interaction	$(\beta\rho)_{jp}$
	SealPressure x Gap interaction	$(\gamma\rho)_{kp}$
	DwellTime x Gap interaction	$(\delta\rho)_{lp}$
	SealTemp x SealPressure x Gap interaction	$(\beta\gamma\rho)_{jkp}$
	SealTemp x DwellTime x Gap interaction	$(\beta\delta\rho)_{jdp}$
	SealPressure x DwellTime x Gap interaction	$(\gamma\delta\rho)_{kdp}$
	Gap x Adhesive interaction	$(\rho\lambda)_{pm}$
	SealTemp x Gap x Adhesive interaction	$(\beta\rho\lambda)_{jpm}$
	SealPressure x Gap x Adhesive interaction	$(\gamma\rho\lambda)_{kpm}$
	DwellTime x Gap x Adhesive interaction	$(\delta\rho\lambda)_{lpm}$
	SealTemp x SealPressure x DwellTime x Gap	$(\beta\gamma\delta\rho)_{jklp}$
	SealTemp x SealPressure x Gap x Adhesive	$(\beta\gamma\rho\lambda)_{jkpm}$
	SealTemp x DwellTime x Gap x Adhesive	$(\beta\delta\rho\lambda)_{jlpm}$
	SealPressure x DwellTime x Gap x Adhesive	$(\gamma\delta\rho\lambda)_{klpm}$
	SealTemp x SealPressure x DwellTime x Gap x Adhesive (Sub-subplot error	$(\beta\gamma\delta\rho\lambda)_{jklpm}$

Table 24. Factor effects for the split-split-plot design for studying effect of seal process parameters on burst pressure

Element	Factor	Effect
Whole plot	Replicates (Packages or blocks)	τ_i
	SealTemp main effect	β_j
	Whole plot error (Replicates x SealTemp)	$(\tau\beta)_{ij}$
Subplot	SealPressure main effect	γ_k
	Replicates x SealPressure interaction	$(\tau\gamma)_{ik}$
	SealTemp x SealPressure interaction	$(\beta\gamma)_{jk}$
	Subplot error (Replicates x SealTemp x SealPressure)	$(\tau\beta\gamma)_{ijk}$
Sub-subplot	DwellTime main effect	δ_l
	Replicates x DwellTime interaction	$(\tau\delta)_{il}$
	SealTemp x DwellTime interaction	$(\beta\delta)_{jl}$
	Replicates x SealTemp x DwellTime interaction	$(\tau\beta\delta)_{ijl}$
	SealPressure x DwellTime interaction	$(\gamma\delta)_{kl}$
	Replicates x SealPressure x DwellTime interaction	$(\tau\gamma\delta)_{ikl}$
	SealTemp x SealPressure x DwellTime interaction	$(\beta\gamma\delta)_{jkl}$
	Replicates x SealTemp x SealPressure x DwellTime interaction	$(\tau\beta\gamma\delta)_{ijkl}$
	Gap main effect	ρ_p
	Replicates x Gap interaction	$(\tau\rho)_{ip}$
	SealTemp x Gap interaction	$(\beta\rho)_{jp}$
	Replicates x SealTemp x Gap interaction	$(\tau\beta\rho)_{ijp}$
	SealPressure x Gap interaction	$(\gamma\rho)_{kp}$
	Replicates x SealPressure x Gap interaction	$(\tau\gamma\rho)_{ikp}$
	DwellTime x Gap interaction	$(\delta\rho)_{lp}$
	Replicates x DwellTime x Gap interaction	$(\tau\delta\rho)_{ilp}$
	SealTemp x SealPressure x Gap interaction	$(\beta\gamma\rho)_{jkp}$
	Replicates x SealTemp x SealPressure x Gap interaction	$(\tau\beta\gamma\rho)_{ijkp}$
	SealTemp x DwellTime x Gap interaction	$(\beta\delta\rho)_{jdp}$
	Replicates x SealTemp x DwellTime x Gap interaction	$(\tau\beta\delta\rho)_{ijdp}$
	SealPressure x DwellTime x Gap interaction	$(\gamma\delta\rho)_{kdp}$
	Replicates x SealPressure x DwellTime x Gap interaction	$(\tau\gamma\delta\rho)_{ikdp}$
	SealTemp x SealPressure x DwellTime x Gap interaction	$(\beta\gamma\delta\rho)_{jklp}$
	Replicates x SealTemp x SealPressure x DwellTime x Gap (Sub-subplot error)	$(\tau\beta\gamma\delta\rho)_{ijklp}$

Analysis

Data collection and processing

The fractional factorial design for studying burst pressure response to SealTemp, SealPressure, DwellTime, LenWidth, TrayArea, and Gap was replicated nine times. The 290° setting proved to be infeasible for five of the trays (PS1, PS2, PS4, PS7, PS9) as the flanges tended to melt at this temperature. This was most likely due to smaller wall thicknesses created during thermoforming. As a result, there were nine missing data points for each of these five trays, yielding 198 packages in the sample instead of 243.

An additional 27 trays were sealed for package PS8 with the CR27 adhesive for evaluation of the effect of Adhesive, yielding a total of 225 packages for burst testing.

Descriptive statistics and graphical analysis

Numerous tables and graphs were produced to summarize the specimen data and aid in the identification of patterns in the data. These analyses are included in several separate appendices.

Table A22-1 in Appendix A22 shows the number of packages tested, grouped by seal setting, gap and adhesive, as well as the mean, standard deviation, minimum and maximum of burst pressure for each group. Process settings for each seal setting are as defined in Table 22.

Table A22-2 in Appendix A22 gives the observed burst pressure for each package tested, as well as the seal setting/gap/adhesive group mean and standard deviation.

Appendix A23 presents a histogram of Burst Location over all packages. This chart shows that over 73% of the burst locations were at one of the corners of the tray. The top five locations were X, W, Y, L, and Z, which comprised over 67% of the samples (location L is next to corner W). This result agrees with the finding in Chapter III that lowest peel strength is near the corners of the tray.

Appendix A24 presents histograms of Burst Location by Package and Adhesive. This presentation reveals that only two packages had no corner burst location. The other seven had 25% to 100% corner burst locations; five packages had 90% and higher corner burst locations. Given the varied lengths, widths, and volumes of the trays, it seems that this finding is generally applicable, and most trays can be expected to have the burst location at or near a corner.

Appendix A25 presents histograms of Burst Location by Seal Setting and Adhesive. The frequencies of burst locations were seen to vary as seal setting varied, but a corner location was still the most frequent at each setting.

Appendix A26 presents histograms of Burst Location by Seal Setting, Gap and Adhesive. Each combination of Seal Setting and Gap is considered as a treatment and referenced by a treatment number (TRT). As gap distance varied within a specific seal setting, burst location frequencies changed. This implies that for a package of a given seal strength, the burst location will be different at different gap distances, so consistency in setting the gap distance is important during process development and subsequent process control.

Regression analysis

The data from this experiment were used to fit linear models of burst pressure response to sealing process factors, restraining plate gap, and tray characteristics. This analysis is described in Chapter VI.

Analysis of effect of adhesive

The fractional factorial design for studying the effect of Adhesive on burst pressure was unreplicated, so the adhesive effect was analyzed using normal probability plots and plots of residuals. There were 54 packages of configuration PS8 in the sample. An initial regression was performed for the burst pressure response on a full model including all main effects and interactions for seal temperature, seal pressure, dwell time, adhesive, and gap distance. The effects from the full-model regression were plotted against normal probability ranks to identify significant effects. A second regression was run with a reduced model including only the significant effects.

The half-normal probability plot of effects in Figure 15 shows that the temperature, dwell, and gap effects were significant for burst pressure; the adhesive effect was not significant. Appendix A36 includes normal and half-normal probability plots of effects for the full model, as well as plots of residuals for the reduced model which includes temperature, dwell time, and gap distance only.

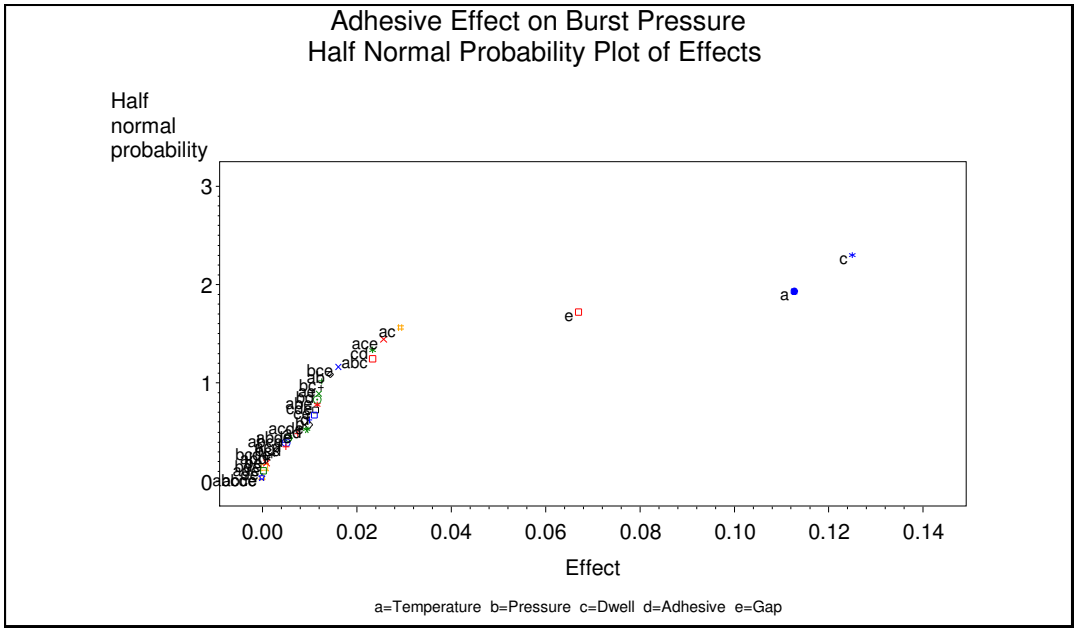

Figure 15. Half-normal probability plot of effects for burst pressure.

Interpretation of results

Burst location for a given package varies with gap distance and sealing process settings, but the majority of packages will burst at one of the corners. Careful attention to test setup and methodology are required in order to achieve consistent test results over time.

There was not a significant difference in the response for the two adhesives tested. Since both adhesives were of the water-based flood-coated adhesive type, it is reasonable that the results were comparable under the conditions tested.

CHAPTER VI

DEVELOPMENT OF AN EMPIRICAL MODEL OF BURST PRESSURE FOR MEDICAL DEVICE TRAYS

Background

Inflation seal-strength (burst pressure) values of lidded trays are affected by characteristics of the packaging materials and by parameters of the package sealing and burst testing processes. In Chapter V an experiment was designed and carried out to collect data for the analysis of the effect of sealing process settings, packaging characteristics and gap distance on burst pressure, using nine representative package configurations. In this chapter an empirical model was developed to predict burst pressure as a function of package characteristics and process parameters, based on the data collected in Chapter V.

Model development

Method

Regression analysis was used to fit a model of burst pressure to the data from the burst pressure experiment presented in Chapter V.

The response variable for the analyses was BurstPressure. The regressors for the analyses were seal temperature, seal pressure, dwell time, tray length-width ratio, tray area, restraining plate gap, tray volume, and tray height. All possible subsets of the regressors—constrained to include temperature, pressure, dwell, gap and volume—were fit. Each of these eight subset regressions was run with and without an intercept term, resulting in sixteen models to be fit and evaluated.

The sixteen regression models were fit using three different groupings of the available study data. One grouping was by adhesive and package. There were nine package configurations in the study, one of which was sealed using both adhesives. The other eight packages were sealed using only one adhesive. Therefore, there were ten adhesive-package subsamples. Within each subsample the sixteen models were fit and compared, and model diagnostics were generated to identify the best models for the subsample.

Another grouping was according to similarities in tray material and shared sealing equipment. This grouping was intended to eliminate unexplained variation that may be due to differences in the tray material or the installation, maintenance, and operation of different sealing equipment. The two groupings were [PS1, PS2, PS4, PS7] and [PS3, PS6]. Within each package group the sixteen models were fit and compared, and model diagnostics were generated to identify the best models for the group.

Finally, the regressions were run using all available samples ungrouped (N=225 packages). This overall dataset comprises packages of nine different sizes—some with slightly different tray materials—sealed with two adhesives on five sealers with various settings of seal temperature, seal pressure, and dwell time. The sixteen models were fit and compared, and model diagnostics were generated to identify the best models for the sample. The variation in the study samples makes them representative of many of the package configurations in use; therefore the resulting model should have broad applicability.

Eight subset models of the regressors were fit using SAS® Proc Reg with the RSQUARE selection criterion. Seven subsets were selected by determining all possible subsets of LenWidth, TrayArea, and TrayHeight and adding SealTemp, SealPressure, DwellTime, Gap and TrayVolume to each subset. The eighth subset includes SealTemp, SealPressure, DwellTime, Gap and TrayVolume only. The full model is shown in Equation 6.1 (3-factor and higher interactions are not listed for the sake of brevity).

$$\begin{aligned}\text{BurstPressure} = {} & \beta_0 + \beta_1\text{SealTemp} + \beta_2\text{SealPressure} + \beta_{12}\text{SealTemp*SealPressure} \\ & + \beta_3\text{DwellTime} + \beta_{13}\text{SealTemp*DwellTime} + \beta_{23}\text{SealPressure*DwellTime} + \beta_4\text{Gap} \\ & + \beta_{14}\text{SealTemp*Gap} + \beta_{24}\text{SealPressure*Gap} + \beta_{34}\text{DwellTime*Gap} + \beta_5\text{TrayVolume} \\ & + \beta_{15}\text{SealTemp*TrayVolume} + \beta_{25}\text{SealPressure*TrayVolume} + \beta_{35}\text{DwellTime*TrayVolume} \\ & + \beta_{45}\text{Gap*TrayVolume} + \beta_6\text{LenWidth} + \beta_{16}\text{SealTemp*LenWidth} + \beta_{26}\text{SealPressure*LenWidth} \\ & + \beta_{36}\text{DwellTime*LenWidth} + \beta_{46}\text{Gap*LenWidth} + \beta_{56}\text{TrayVolume*LenWidth} + \beta_7\text{TrayArea} \\ & + \beta_{17}\text{SealTemp*TrayArea} + \beta_{27}\text{SealPressure*TrayArea} + \beta_{37}\text{DwellTime*TrayArea} \\ & + \beta_{47}\text{Gap*TrayArea} + \beta_{57}\text{TrayVolume*TrayArea} + \beta_{67}\text{LenWidth*TrayArea} + \beta_8\text{TrayHeight} \\ & + \beta_{18}\text{SealTemp*TrayHeight} + \beta_{28}\text{SealPressure*TrayHeight} + \beta_{38}\text{DwellTime*TrayHeight} \\ & + \beta_{48}\text{Gap*TrayHeight} + \beta_{58}\text{TrayVolume*TrayHeight} + \beta_{68}\text{LenWidth*TrayHeight} \\ & + \beta_{78}\text{TrayArea*TrayHeight} + \text{higher-order interactions} + \varepsilon \end{aligned} \quad (6.1)$$

For ease of reference, each model configuration was given a name, as shown in Table 25. Each model was fit with β_0 estimated, and with β_0 assumed equal to zero (no intercept model).

Table 25. Model configurations for regression of burst pressure on sealing, package, and burst test parameters

Model Name	Response Variable	Independent Variables				Grouping
BM1	BurstPressure	SealTemp TrayVolume	SealPressure LenWidth	DwellTime TrayArea	Gap TrayHeight	Adhesive-Package
BM2	BurstPressure	SealTemp TrayVolume	SealPressure LenWidth	DwellTime TrayArea	Gap TrayHeight	Overall
BM3	BurstPressure	SealTemp TrayVolume	SealPressure LenWidth	DwellTime TrayArea	Gap TrayHeight	Package group

For each model, R^2, adjusted R^2, Mallow's C_p, Akaike's Information Criterion (AIC), prediction error sum of squares (PRESS), and prediction R^2 statistics were calculated. Equations for AIC, adjusted R^2, PRESS and C_p are presented in Equations 4.2 through 4.6 along with accompanying discussions of these statistics.

Within each subsample or group, the models were ranked first by AIC, with lower AIC scores indicating better quality models, then by highest adjusted R^2. The model that was ranked number one by AIC was considered the best model within the group, unless the model had a negative adjusted R^2 or prediction R^2. In this case, the highest ranking model with positive R^2 statistics was considered the best model.

Results

Several regression analyses were completed separately for adhesive-package groups, package groups, and the overall sample. Externally studentized residuals were plotted against the regressors and predicted response. There were no obvious patterns in these plots that would indicate severe changes in variance as the regressor or predicted response variables change. Normal probability plots of the residuals indicated that the errors were approximately normally distributed.

The models that ranked within the top five within each group according to AIC are summarized in Appendices A27, A28, and A29. Each summary includes a table with model parameter estimates, fit statistics, and model diagnostics and a table with ANOVA statistics for the regression.

Analysis by adhesive and package

Appendix A27 includes a summary of the regression analyses by Adhesive and Package. A review of these data reveals that the top five ranking models all had favorable results for the Cp, PRESS, and RMSE model diagnostics. Cp was equal to p, which indicates a lack of bias. PRESS was very close to SSE, and RMSE was low. R^2 and adjusted R^2 were close, so no overfitting was indicated. All of the models had adjusted R^2 values of .93 to .99 and prediction R^2 values of .92 to .99.

None of the top ranked models included the intercept term. It is plausible that regression through the origin (RTO) would be applicable to the response variable studied, since the burst pressure would be expected to equal zero if the temperature, pressure, and dwell time are zero. As a check whether RTO

might be appropriate, burst pressure was plotted against three parameter levels: 'Low' = SealTemp 240/SealPressure 75/DwellTime 3, 'Med' = SealTemp 260/SealPressure 85/DwellTime 4.5, and 'High" = SealTemp 290/SealPressure 95/DwellTime 6.5. These plots are included in Appendix A21, and indicate that the burst pressure response is approximately linear in the parameter levels. For most of the packages the line of best fit appears to pass through the origin, so it is possible that the RTO models may provide acceptable results in application.

Seal Temperature and Dwell Time were significant in all models except the PS2 and PS9 models. Gap was significant in all models except the PS9 models. Tray Volume was significant in the models for PS3, PS5, PS7, and PS8. Seal Pressure, Tray Area, Length-Width ratio, and Tray Height were not significant in any of the models. It is interesting that the PS9 models had no parameters significant at $p<=.05$. All of the p-values were .32 and higher. It is also interesting that the PS2 models had only one significant parameter, which was Gap. The p-value for Dwell Time was .10 and the p-value for Seal Temperature was .13. Gap was the most important parameter in all models, with coefficients 27 to 216 times the coefficients of temperature and coefficients eight to 30 times the coefficients of Dwell Time.

Table 26 summarizes the coefficients and adjusted R^2 values among the 1st ranked models. The coefficients for Seal Temperature and Seal Pressure were very consistent across the packages, as shown in Table 26. There was considerably more variation in the Dwell Time coefficients, and pronounced differences in the Gap coefficients.

Table 27 lists the details for the highest ranking models based on AIC score.

Table 26. Summary of parameters for adhesive-package burst pressure regression models with lowest AIC score

Dependent Variable	Parameter	Minimum Value	Maximum Value	Range
Burst Pressure	Intercept	0	0	0
	Seal Temperature	0	.02	.02
	Seal Pressure	-.01	.01	.02
	Dwell Time	.04	.21	.17
	Gap	-4.32	-.19	4.13
	Tray Volume	-.34	.03	.37
	Length-Width	0	0	0
	Tray Height	0	0	0
	Tray Area	0	0	0
	Adjusted R^2	.93	.99	.06
	Prediction R^2	.92	.99	.07

Table 27. Best models for burst pressure by adhesive and package

Dependent Variable	Adhesive	Package	Model	Model ID	Intercept	Seal Temp	Seal Pressure	Dwell Time	Gap	Tray Height	Tray Volume	Len Width	Tray Area	Adjusted R^2	Prediction R^2	N	AIC	MSE	Selected by
BurstPressure	Amcor	PS1	BM1	BM1-1	.	0.02	0.01	0.21	-2.29	.	-0.34	.	.	0.98	0.98	18	-30.08	0.15	A and R
		PS2	BM1	BM1-1	.	0.02	-0.01	0.14	-4.32	.	-0.04	.	.	0.95	0.93	18	-22.77	0.22	A and R
		PS3	BM1	BM1-1	.	0.02	0.01	0.15	-1.43	.	-0.26	.	.	0.98	0.98	27	-72.37	0.06	A and R
		PS4	BM1	BM1-1	.	0.01	-0.00	0.08	-0.67	.	-0.09	.	.	0.96	0.95	18	-54.35	0.04	A and R
		PS5	BM1	BM1-1	.	0.01	-0.00	0.12	-1.61	.	-0.10	.	.	0.99	0.99	27	-88.76	0.03	A and R
		PS6	BM1	BM1-1	.	0.01	0.00	0.12	-0.96	.	-0.04	.	.	0.98	0.97	27	-76.69	0.05	A and R
		PS7	BM1	BM1-1	.	0.01	0.00	0.07	-0.60	.	-0.06	.	.	0.99	0.99	18	-93.49	0.00	A and R
		PS8	BM1	BM1-1	.	0.00	0.00	0.06	-0.27	.	-0.02	.	.	0.98	0.98	27	-149.31	0.00	A and R
		PS9	BM1	BM1-1	.	-0.00	-0.01	0.04	-0.19	.	0.03	.	.	0.93	0.92	18	-45.98	0.06	A and R
	Perfecseal	PS8	BM1	BM1-1	.	0.01	-0.00	0.08	-0.27	.	-0.02	.	.	0.97	0.96	27	-131.45	0.01	A and R

Analysis by package group

Appendix A28 includes a summary of the regression analyses by Package groups. A review of these data reveals that the top five ranking models all had favorable results for the Cp, PRESS, and RMSE model diagnostics. Cp was equal to p, which indicates a lack of bias. PRESS was very close to SSE, and RMSE was low. R^2 and adjusted R^2 were close, so no overfitting was indicated. All models had adjusted R^2 values from .82 to .97 and prediction R^2 values from .79 to .97.

Only two of the top ranked models included the intercept term, the 4th and 5th ranked models for package group [PS1 PS2 PS4 PS7]; the intercept was significant at p<=.05. Neither of the models with lowest AIC score contained the intercept term.

Seal Temperature, Dwell Time, and Gap were significant in all models. Tray Volume and Tray Area were significant in the models for package group [PS1 PS2 PS4 PS7]. Length-Width ratio was significant only in the 4th and 5th ranked models for package group [PS1 PS2 PS4 PS7]. Tray Height was significant only in the 1st through 3rd ranked models for package group [PS1 PS2 PS4 PS7]. Seal Pressure was not significant in any of the models. Gap was the most important parameter in all models, with coefficients 98 to 120 times the coefficients of Seal Temperature and coefficients eight to 15 times the coefficients of Dwell Time.

Table 28 summarizes the coefficients and adjusted R^2 values among the 1st ranked models. The coefficients for Seal Temperature, Seal Pressure, and Dwell Time were very consistent between the package groups, as shown in Table 28. There was considerably more variation in the Tray Volume, Gap and Tray Height coefficients. The coefficient for Tray Height was almost as large as the Gap coefficient in the model for group [PS1 PS2 PS4 PS7], but did not appear in the model for the other group. The ranges of all of the parameter coefficients and R^2 values were lower for the package group analysis than for the adhesive-package analysis.

The adjusted R^2 values for group [PS3 PS6] were equivalent to the R^2 values for the individual packages. The adjusted R^2 values for group [PS1 PS2 PS4 PS7] were slightly lower than the R^2 values for the individual packages, but the differences were not as large as those seen in the peel force regression.

Table 29 lists the details for the highest ranking models based on AIC score.

Table 28. Summary of parameters for package group burst pressure regression models with lowest AIC score

Dependent Variable	Parameter	Minimum Value	Maximum Value	Range
Burst Pressure	Intercept	0	0	0
	Seal Temperature	.01	.02	.01
	Seal Pressure	.00	.01	.01
	Dwell Time	.13	.14	.01
	Gap	-1.96	-1.20	.76
	Tray Volume	-.02	.09	.11
	Length-Width	0	0	0
	Tray Height	-1.22	0	1.22
	Tray Area	-.04	-.04	0
	Adjusted R^2	.94	.97	.03
	Prediction R^2	.94	.97	.03

Table 29. Best models for burst pressure by package group

Dependent Variable	Package Group	Model	Model ID	Intercept	Seal Temp	Seal Pressure	Dwell Time	Gap	Tray Height	Tray Volume	Len Width	Tray Area	Adjusted R^2	Prediction R^2	N	AIC	MSE	AIC rank	Selected by
BurstPressure	PS1 PS2 PS4 PS7	BM3	BM3-1	.	0.02	0.00	0.13	-1.96	-1.22	0.09	.	-0.04	0.94	0.94	72	-108.03	0.20	1	A and R
	PS3 PS6	BM3	BM3-1	.	0.01	0.01	0.14	-1.20	.	-0.02	.	-0.04	0.97	0.97	54	-133.87	0.08	1	A and R

Table 30. Best model for burst pressure over all packages

Dependent Variable	Model	Model ID	Intercept	Seal Temp	Seal Pressure	Dwell Time	Gap	Tray Height	Tray Volume	Len Width	Tray Area	Adjusted R^2	Prediction R^2	N	AIC	MSE	AIC rank	Selected by
BurstPressure	BM2	BM2-1	1.25	0.01	0.00	0.11	-1.16	-1.38	0.07	.	-0.03	0.81	0.80	225	-436.09	0.14	1	A and R

Analysis over all packages

Appendix A29 includes a summary of the regression analyses over all packages. A review of these data reveals that the top five ranking models all had favorable results for the Cp, PRESS, and RMSE model diagnostics. Cp was equal to p, which indicates a lack of bias. PRESS was very close to SSE, and RMSE was low. R^2 and adjusted R^2 were close, so no overfitting was indicated.

The four models that were highest ranked by AIC included the intercept term. In each of these models, the intercept was significant at p-value <= .05. The models that included the intercept term had lower R^2 values than the one model that was fit through the origin, but the differences were not as large as those seen in the peel force regressions. The 5th ranked model had an adjusted R^2 of .94, while the four intercept models had adjusted R^2 values of .81.

Seal Temperature, Dwell Time, Gap, Tray Volume, Tray Area, and Tray Height were significant in all models. Seal Pressure was significant only in the 5th ranked model. Length-Width ratio was not significant in any model. Tray Height was the most important parameter in the models, followed closely by Gap. The Tray Height coefficient was 1.08 to 1.14 times the Gap coefficient. The coefficients of Tray Height were 11 to 138 times the coefficients of the other parameters. The coefficients of Gap were ten to 116 times the coefficients of the other parameters.

Table 30 lists details for the highest ranking model based on AIC score, and Table 31 summarizes the coefficients and adjusted R^2 values.

Table 31. Summary of parameters for overall burst pressure regression model with lowest AIC score

Dependent Variable	Parameter	Value
Burst Pressure	Intercept	1.25
	Seal Temperature	.01
	Seal Pressure	0
	Dwell Time	.11
	Gap	-1.16
	Tray Volume	.07
	Length-Width	0
	Tray Height	-1.38
	Tray Area	-.03
	Adjusted R^2	.81
	Prediction R^2	.80

The 5th ranked model was a no-intercept regression model which had an adjusted R^2 of .94, and an AIC score just 4.94 above the AIC of the 1st ranked model. Table 32 summarizes the coefficients and adjusted R^2 value for this model. The predictive equation based on this RTO model is given in Table 33.

Table 32. Summary of parameters for overall burst pressure regression model with lowest AIC score and adjusted $R^2 > .90$

Dependent Variable	Parameter	Value
Burst Pressure	Intercept	0
	Seal Temperature	.01
	Seal Pressure	.01
	Dwell Time	.11
	Gap	-1.12
	Tray Volume	.06
	Length-Width	-.03
	Tray Height	-1.21
	Tray Area	-.03
	Adjusted R^2	.94
	Prediction R^2	.94

Table 33. Predictive equation for burst pressure based on sealing, package, and burst test parameters

Equation	Adjusted R^2	Prediction R^2
Burst Pressure = 0.01*Seal Temperature + 0.01*Seal Pressure + 0.11*Dwell Time – 1.12*Gap + 0.06*Tray Volume – 0.03*Length-Width Ratio –1.21*Tray Height – 0.03*Tray Area	.94	.94

Interpretation of results

In the adhesive-package and package-group analyses the models selected by AIC did not include an intercept term. The selected model in the overall analysis included an intercept, and had an adjusted R^2 value of .80. The fifth-ranked model was a no-intercept model with an adjusted R^2 value of .94, and was selected as the best model. The RTO model would be applicable if it is believed that the response should be zero if the three parameters are zero, and that the linear relationship is continuous from the study range to the origin. The plots presented in Appendix A21 support the possibility that RTO models may provide acceptable results in application, but this needs to be confirmed by further investigation.

The variability in the coefficients of Gap and Tray Height in the adhesive-package and package group analysis was too high for those models to be used as the basis for generally applicable prediction equations. However, the selected model developed from the analysis over all packages should be generally applicable and had a high R^2 value.

The coefficient for Gap is the largest and is negative in sign, so as Gap decreases pressure increases. This agrees with the principle reported in the literature that restrained packages burst at higher pressures. Decreasing the gap distance corresponds to more restraint, and the equation would produce a higher burst pressure. This is because when the package is restrained the forces within the package are distributed directly onto the seal area rather than toward expanding the lid. The higher force per unit area of seal creates a higher burst pressure.

Based on the coefficients for tray height and tray area, the equation would predict lower burst pressures for packages with larger areas, as is also reported in the literature. The equation would also predict lower burst pressures for packages with higher length to width ratios. The equation assigns a positive coefficient to seal temperature, seal pressure and dwell time. These results are as expected, since temperature, pressure, and dwell are the primary controlled inputs that produce the tray seal.

The selected burst pressure predictive equation has high adjusted R^2 value and prediction R^2 values The equation explains a high percentage of the variability in the study data and also can be expected to explain a high percentage of the variability in predicting new response values.

CHAPTER VII

EVALUATION OF AGREEMENT BETWEEN LOWEST PEEL FORCE LOCATION AND BURST LOCATION

Background

Inflation seal strength (burst pressure) and tensile seal strength (peel force) are similarly affected by characteristics of the packaging materials and package sealing process parameters. The ability to use burst location to identify the location of lowest peel strength would allow testers to reduce the number of specimens that would need to be cut when conducting peel testing. It was shown in Chapter V that the burst location for a specific package geometry changes based on seal process settings and restraining plate gap distance. A comparative analysis was performed to assess the ability to identify the locations of lowest peak peel force and lowest average peel force based on an observed burst location.

Analysis

The comparative analysis was completed using the 9-package burst pressure data set from Chapter V and the 9-package peel force data set from Chapter III. One hundred twenty-four (124) tray samples from the burst pressure data set were matched with the trays from the peel force data set that were sealed under the same conditions. The locations of lowest peak and average peel forces were identified for each tray that was peel tested. Lowest peel force locations were compared to burst locations to determine whether burst location served as an indicator of lowest peel force location.

Table A30-1 in Appendix A30 gives the detailed data for the matched packages used in the burst pressure to peel force comparisons. The table includes package identification, burst pressure value, burst test and seal process parameters, peak and average peel forces, burst and peel locations, and measures of agreement between burst and peel locations.

Results

Match percentages were calculated over all packages and for each Adhesive/Package group separately. Table 34 summarizes the percentages of agreement between burst location and lowest peak peel force location and lowest average peel force location. Overall, average peel force location tended to match the burst location more frequently than lowest peak peel force location. For 60% of the packages, the lowest average force location had a higher match percentage than the lowest peak force location. For three of the packages match percentages at the average force location were as high as 67%. Over all packages, the lowest average force location matched the burst location for 34% of the samples, while lowest peak force location matched for 27% of the samples. This may indicate that average peel force should be used as a more reliable measure of minimum package seal strength.

Table 34. Agreement between burst location and lowest peel force locations – overall and by adhesive and package

		% of Locations Matching Burst Location			
Adhesive	**Package**	**Lowest Avg Force Location**	**Lowest Peak Force Location**	**Lowest Avg Force Location**	**Lowest Peak Force Location**
Amcor	PS1	30	10	34	27
Amcor	PS2	0	30		
Amcor	PS3	33	40		
Amcor	PS4	30	20		
Amcor	PS5	67	67		
Amcor	PS6	67	53		
Amcor	PS7	0	0		
Amcor	PS8	13	7		
Amcor	PS9	67	22		
Perfecseal	PS8	20	7		

Match percentages were also calculated for each Adhesive/Package group within gap level. Table 35 summarizes the percentages of agreement between burst location and lowest peak peel force location and lowest average peel force location. A comparison of Table 35 with Table 34 reveals that the match percentages are higher for all packages when calculated within gap level. At all gap levels, average peel force location matched the burst location more frequently than lowest peak peel force location, as was seen in the overall analysis. No gap level appeared to be clearly better than another for producing higher match percentages.

Interpretation of results

Burst location was able to identify the average peel force location more accurately than the peak peel force location. Since average force is lower than peak peel force, the location of lowest average force can be considered as the minimum seal strength location. The burst location was able to identify this lowest seal strength location for 34% of packages overall. Since the burst location has been shown to vary as gap distance changes, the low overall match percentage is probably due to varying gap level.

Calculation of match percentages within gap levels resulted in higher percentages for all packages, with 60% of packages having match percentages of 67% to 100%. Neither gap distance emerged as clearly better for matching burst location, so the gap distance should be selected for each package during test planning. The gap distance should be selected with consideration of the clearance that the package has when enclosed in its sterilization packaging. At a fixed gap level for a specific package, the current results indicate that burst location may be able to identify the lowest peel strength location in a high percentage of cases.

Table 35. Agreement between burst location and lowest peel force locations – by adhesive and package within gap level

Gap=.25

		% of Locations Matching Burst Location	
Adhesive	Package	Lowest Avg Force Location	Lowest Peak Force Location
Amcor	PS1	0	0
Amcor	PS2	0	20
Amcor	PS3	0	0
Amcor	PS4	40	20
Amcor	PS5	83	83
Amcor	PS6	0	0
Amcor	PS7	0	0
Amcor	PS8	0	0
Amcor	PS9	75	25
Perfecseal	PS8	0	0

Gap=.50

		% of Locations Matching Burst Location	
Adhesive	Package	Lowest Avg Force Location	Lowest Peak Force Location
Amcor	PS1	20	20
Amcor	PS2	0	0
Amcor	PS3	100	100
Amcor	PS4	33	33
Amcor	PS5	67	33
Amcor	PS6	67	67
Amcor	PS7	0	0
Amcor	PS8	17	17
Amcor	PS9	67	33
Perfecseal	PS8	33	0

Gap=.75

		% of Locations Matching Burst Location	
Adhesive	Package	Lowest Avg Force Location	Lowest Peak Force Location
Amcor	PS1	67	0
Amcor	PS2	0	100
Amcor	PS3	33	50
Amcor	PS4	0	0
Amcor	PS5	50	67
Amcor	PS6	100	67
Amcor	PS7	0	0
Amcor	PS8	17	0
Amcor	PS9	50	0
Perfecseal	PS8	17	17

CHAPTER VIII

DEVELOPMENT OF EMPIRICAL MODELS TO PREDICT PEEL FORCE FROM BURST PRESSURE

Background

Inflation seal strength (burst pressure) and tensile seal strength (peel force) are similarly affected by characteristics of the packaging materials and package sealing process parameters. In Chapter III and Chapter V experiments were designed and carried out to collect data for the analysis of the effect of packaging characteristics and process settings on peel force and burst pressure, using nine representative package configurations. In this chapter empirical models were developed to predict peel force as a function of restraining plate gap distance and observed burst pressure, based on the data collected in Chapter III and Chapter V.

Model development

Method

Regression analysis was used to fit predictive models using the 9-package burst pressure data set from Chapter V and the 9-package peel force data set from Chapter III. One hundred twenty-four (124) tray samples from the burst pressure data set were matched with the trays from the peel force data set that were sealed under the same conditions.

Regression was performed for four different peel force response variables: (1)peak peel force of the specimen that matched the burst location, (2)average peel force of the specimen that matched the burst location, (3)peak peel force of the specimen that had the lowest peak peel force within the tray, and (4) average peel force of the specimen that had the lowest average peel force within the tray.

The regressors for the analyses were burst pressure and restraining plate gap distance, entered into the models as BurstPressure*Gap, and individually as Burst Pressure and Gap. The three possible subsets of Burst Pressure and Gap, along with the multiplicative regressor yielded four possible subsets for

regression. Each of these four subset regressions was run with and without an intercept term, resulting in eight models to be evaluated for each peel force response, and a total of 32 regression models fit.

The eight regression models were fit for each response variable using three different groupings of the available study data. One grouping was by adhesive and package. There were nine package configurations in the study, one of which was sealed using both adhesives. The other eight packages were sealed using only one adhesive. Therefore, there were ten adhesive-package subsamples. Within each subsample the eight models were fit and compared for each peel force response, and model diagnostics were generated to identify the best models for the subsample.

Another grouping was according to similarities in tray material and shared sealing equipment. This grouping was intended to eliminate unexplained variation that may be due to differences in the tray material or the installation, maintenance, and operation of different sealing equipment. The two groupings were [PS1, PS2, PS4, PS7] and [PS3, PS6]. Within each package group the eight models were fit and compared for each peel force response, and model diagnostics were generated to identify the best models for the group.

Finally, the regressions were run using all available samples ungrouped (N=124 packages). This overall dataset comprises packages of nine different sizes—some with slightly different tray materials—sealed with two adhesives on five sealers with various settings of seal temperature, seal pressure, and dwell time. The eight models were fit and compared for each peel force response, and model diagnostics were generated to identify the best models for the sample. The variation in the study samples makes them representative of many of the package configurations in use; therefore the resulting model should have broad applicability.

The four models shown in Equations 8.1 through 8.4 were fit using SAS® Proc Reg with the RSQUARE selection criterion.

$$PeelForce = \beta_0 + \beta_1 BurstPressure + \beta_2 Gap + \varepsilon \quad (8.1)$$

$$PeelForce = \beta_0 + \beta_1 BurstPressure*Gap + \varepsilon \quad (8.2)$$

$$PeelForce = \beta_0 + \beta_1 BurstPressure + \varepsilon \quad (8.3)$$

$$PeelForce = \beta_0 + \beta_1 Gap + \varepsilon \quad (8.4)$$

The PeelForce term took on each of the four peel force responses described above. For ease of reference, each model configuration was given a name, as shown in Table 36. Each model was fit with β_0 estimated, and with β_0 assumed equal to zero (no intercept model).

Table 36. Model configurations for regression of peel force on burst pressure

Model Name	Response Variable	Independent Variables	Grouping
M1	PeakForce_at_BurstLoc	BurstPressure*Gap	Adhesive-Package
M2	AvgForce_at_BurstLoc	BurstPressure*Gap	Adhesive-Package
M3	LowestPeakForce	BurstPressure*Gap	Adhesive-Package
M4	LowestAvgForce	BurstPressure*Gap	Adhesive-Package
M5	PeakForce_at_BurstLoc	BurstPressure Gap	Adhesive-Package
M6	AvgForce_at_BurstLoc	BurstPressure Gap	Adhesive-Package
M7	LowestPeakForce	BurstPressure Gap	Adhesive-Package
M8	LowestAvgForce	BurstPressure Gap	Adhesive-Package
M9	PeakForce_at_BurstLoc	BurstPressure*Gap	Overall
M10	AvgForce_at_BurstLoc	BurstPressure*Gap	Overall
M11	LowestPeakForce	BurstPressure*Gap	Overall
M12	LowestAvgForce	BurstPressure*Gap	Overall
M13	PeakForce_at_BurstLoc	BurstPressure Gap	Overall
M14	AvgForce_at_BurstLoc	BurstPressure Gap	Overall
M15	LowestPeakForce	BurstPressure Gap	Overall
M16	LowestAvgForce	BurstPressure Gap	Overall
M17	PeakForce_at_BurstLoc	BurstPressure*Gap	Package group
M18	AvgForce_at_BurstLoc	BurstPressure*Gap	Package group
M19	LowestPeakForce	BurstPressure*Gap	Package group
M20	LowestAvgForce	BurstPressure*Gap	Package group
M21	PeakForce_at_BurstLoc	BurstPressure Gap	Package group
M22	AvgForce_at_BurstLoc	BurstPressure Gap	Package group
M23	LowestPeakForce	BurstPressure Gap	Package group
M24	LowestAvgForce	BurstPressure Gap	Package group

For each model, R^2, adjusted R^2, Mallow's Cp, Akaike's Information Criterion (AIC), prediction error sum of squares (PRESS), and prediction R^2 statistics were calculated. Equations for AIC, adjusted R^2, PRESS and C_p are presented in Equations 4.2 through 4.6 along with accompanying discussions of these statistics.

Within each subsample or group, the models were ranked by AIC, with lower AIC scores indicating better quality models. The model that was ranked number one by AIC was considered the best model within the group, unless the model had a negative adjusted R^2 or prediction R^2. In this case, the highest ranking model with positive R^2 statistics was considered the best model.

Results

Several regression analyses were completed separately for adhesive-package groups, package groups, and the overall sample. Externally studentized residuals were plotted against the regressors and predicted responses. There were no obvious patterns in these plots that would indicate severe changes in variance as the regressor or predicted response variables change. Normal probability plots of the residuals indicated that the errors were approximately normally distributed.

The models that ranked within the top five within each group according to AIC are summarized in Appendices A31, A32, and A33. Each summary includes a table with model parameter estimates, fit statistics, and model diagnostics and a table with ANOVA statistics for the regression.

Analysis by adhesive and package

Appendix A31 includes a summary of the regression analyses by Adhesive and Package. Tables 37 and 38 summarize the coefficients and adjusted R^2 values among the 1st ranked models with additive Burst Pressure and Gap terms and a multiplicative Burst Pressure*Gap term, respectively.

There was significant variability in the Burst Pressure and Gap coefficients, with the variability for peak force at burst location models much higher than the variability for models of the other three response variables. The coefficient for Gap was much larger than the coefficient for Burst Pressure.

The best models as determined by lowest AIC and highest adjusted R^2 are summarized in Tables 39 and 40 for peak and average peel force at the burst location and in Tables 41 and 42 for lowest peak peel force and lowest average peel force within the package.

Table 37. Summary of parameters for adhesive-package burst pressure regression models with lowest AIC score and highest adjusted R^2 with burst pressure and gap terms

Dependent Variable	Parameter	Minimum Value	Maximum Value	Range
Peak Force at Burst Location	Intercept	0	0	0
	Burst Pressure	.25	2.72	2.47
	Gap	0	5.40	5.40
	Adjusted R^2	.91	.98	.07
	Prediction R^2	.86	.98	.12
Average Force at Burst Location	Intercept	0	0	0
	Burst Pressure	.20	1.14	.94
	Gap	.73	4.57	3.84
	Adjusted R^2	.90	.98	.08
	Prediction R^2	.84	.96	.12
Lowest Peak Force	Intercept	0	0	0
	Burst Pressure	.18	.98	.80
	Gap	1.05	4.37	3.32
	Adjusted R^2	.90	.97	.07
	Prediction R^2	.83	.96	.13
Lowest Average Force	Intercept	0	0	0
	Burst Pressure	.14	.48	.34
	Gap	0	3.84	3.84
	Adjusted R^2	.89	.96	.07
	Prediction R^2	.83	.96	.13

Table 38. Summary of parameters for adhesive-package burst pressure regression models with lowest AIC score and highest adjusted R^2 with burst pressure*gap term

Dependent Variable	Parameter	Minimum Value	Maximum Value	Range
Peak Force at Burst Location	Intercept	0	0	0
	Burst Pressure * Gap	1.57	2.96	1.39
	Adjusted R^2	.89	.99	.10
	Prediction R^2	.88	.99	.11
Average Force at Burst Location	Intercept	0	0	0
	Burst Pressure * Gap	1.12	2.82	1.70
	Adjusted R^2	.80	.98	.18
	Prediction R^2	.78	.98	.20
Lowest Peak Force	Intercept	0	0	0
	Burst Pressure * Gap	1.02	3.15	2.13
	Adjusted R^2	.84	.98	.14
	Prediction R^2	.83	.98	.15
Lowest Average Force	Intercept	0	0	0
	Burst Pressure * Gap	.78	2.46	1.68
	Adjusted R^2	.80	.96	.16
	Prediction R^2	.80	.96	.16

Table 39. Best models for predicting peak and average force at burst location from burst pressure and gap by adhesive and package

Dependent Variable	Adhesive	Package	Model	Model ID	Intercept	Burst Pressure	Gap	Adjusted R^2	Prediction R^2	N	AIC	MSE	AIC rank	Selected by
PeakForce_at_BurstLoc	Amcor	PS1	M5	M5-1	.	0.25	3.97	0.98	0.98	10	-4.47	0.54	1	A and R
		PS3	M5	M5-1	.	0.53	1.11	0.98	0.97	15	-6.17	0.59	1	A and R
		PS5	M5	M5-2	.	0.37	1.79	0.95	0.95	15	-1.83	0.78	2	R
		PS6	M5	M5-1	.	0.53	2.73	0.93	0.93	15	8.25	1.53	1	A and R
		PS7	M5	M5-2	.	1.35	5.40	0.97	0.96	10	2.58	1.08	2	A and R
		PS8	M5	M5-1	.	2.43	.	0.92	0.92	15	8.53	1.66	1	A and R
		PS9	M5	M5-4	.	0.75	4.66	0.91	0.86	9	10.27	2.58	4	A and R
	Perfecseal	PS8	M5	M5-1	.	2.72	.	0.92	0.91	15	14.36	2.44	1	A and R
AvgForce_at_BurstLoc	Amcor	PS1	M6	M6-1	.	0.20	2.79	0.97	0.96	10	-4.86	0.52	1	A and R
		PS3	M6	M6-1	.	0.46	0.73	0.97	0.95	15	-6.34	0.58	1	A and R
		PS5	M6	M6-2	.	0.29	1.42	0.95	0.95	15	-8.66	0.50	2	R
		PS7	M6	M6-2	.	1.14	4.57	0.98	0.96	10	-1.14	0.75	2	A and R
		PS9	M6	M6-4	.	0.54	3.84	0.90	0.84	9	7.00	1.79	4	A and R

Table 40. Best models for predicting peak and average force at burst location from burst pressure*gap by adhesive and package

Dependent Variable	Adhesive	Package	Model	Model ID	Intercept	BPxGap	Adjusted R^2	Prediction R^2	N	AIC	MSE	AIC rank	Selected by
PeakForce_at_BurstLoc	Amcor	PS2	M1	M1-1	.	1.57	0.99	0.99	10	-9.91	0.34	1	A and R
		PS4	M1	M1-2	.	2.96	0.89	0.88	10	12.93	3.31	2	A and R
AvgForce_at_BurstLoc	Amcor	PS2	M2	M2-1	.	1.33	0.98	0.98	10	-6.82	0.46	1	A and R
		PS4	M2	M2-2	.	2.17	0.88	0.87	10	8.13	2.05	2	A and R
		PS6	M2	M2-1	.	1.12	0.86	0.85	15	12.07	2.10	1	A and R
		PS8	M2	M2-1	.	2.71	0.84	0.82	15	7.20	1.52	1	A and R
	Perfecseal	PS8	M2	M2-1	.	2.82	0.80	0.78	15	14.46	2.46	1	A and R

Table 41. Best models for predicting lowest peak and lowest average force from burst pressure and gap by adhesive and package

Dependent Variable	Adhesive	Package	Model	Model ID	Intercept	Burst Pressure	Gap	Adjusted R^2	Prediction R^2	N	AIC	MSE	AIC rank	Selected by
LowPeakForce	Amcor	PS1	M7	M7-1	.	0.18	3.87	0.96	0.95	10	-2.27	0.67	1	A and R
		PS3	M7	M7-1	.	0.48	1.05	0.97	0.96	15	-7.86	0.52	1	A and R
		PS7	M7	M7-2	.	0.98	3.91	0.97	0.95	10	-3.12	0.61	2	A and R
		PS9	M7	M7-4	.	0.65	4.37	0.90	0.83	9	9.49	2.37	4	A and R
LowAvgForce	Amcor	PS1	M8	M8-1	.	0.14	2.72	0.96	0.94	10	-7.08	0.41	1	A and R
		PS3	M8	M8-1	.	0.46	.	0.96	0.96	15	-8.82	0.52	1	A and R
		PS4	M8	M8-2	.	0.48	3.28	0.95	0.95	10	-3.28	0.60	2	A and R
		PS9	M8	M8-4	.	0.47	3.84	0.89	0.83	9	5.91	1.59	4	A and R

Table 42. Best models for predicting lowest peak and lowest average force from burst pressure*gap by adhesive and package

Dependent Variable	Adhesive	Package	Model	Model ID	Intercept	BPxGap	Adjusted R^2	Prediction R^2	N	AIC	MSE	AIC rank	Selected by
LowPeakForce	Amcor	PS2	M3	M3-2	.	1.36	0.98	0.98	10	-10.15	0.33	2	R
		PS4	M3	M3-2	.	2.64	0.90	0.89	10	10.33	2.56	2	A and R
		PS5	M3	M3-1	.	1.02	0.87	0.87	15	11.17	1.97	1	A and R
		PS6	M3	M3-1	.	1.30	0.91	0.90	15	9.89	1.81	1	A and R
		PS8	M3	M3-1	.	2.89	0.88	0.88	15	4.08	1.23	1	A and R
		PS8	M3	M3-1	.	3.15	0.84	0.83	15	13.39	2.29	1	A and R
LowAvgForce	Amcor	PS2	M4	M4-1	.	1.06	0.96	0.96	10	-5.68	0.52	1	A and R
		PS5	M4	M4-1	.	0.78	0.88	0.87	15	2.67	1.12	1	A and R
		PS6	M4	M4-1	.	1.06	0.90	0.89	15	4.74	1.29	1	A and R
		PS7	M4	M4-2	.	2.46	0.92	0.91	10	-0.44	0.87	2	A and R
		PS8	M4	M4-1	.	2.14	0.84	0.83	15	0.25	0.95	1	A and R
		PS8	M4	M4-1	.	2.27	0.80	0.80	15	7.64	1.56	1	A and R

Analysis by package group

Appendix A32 includes a summary of the regression analyses by package groups. The multiplicative BurstPressure*Gap term did not appear in any models with adjusted R^2 >.79. The best models as determined by lowest AIC and highest adjusted R^2 are summarized in Tables 43 and 44.

The adjusted R^2 values for these models range from .86 to .95, and prediction R^2 values range from .86 to .94.

The coefficients for Burst Pressure for the two package groups were very close, with differences of .31 for peak force at burst location, .29 for average force at burst location, .27 for lowest peak force, and .25 for lowest average force.

The coefficients for Gap were more variable, with differences of 5.43 for peak force at burst location, 4.69 for average force at burst location, 3.83 for lowest peak force, and 2.54 for lowest average force. The variability in Gap does not allow the development of general predictive equations from these models.

Analysis over all packages

Appendix A33 includes a summary of the regression analyses over all packages. The multiplicative BurstPressure*Gap term did not appear in any models with adjusted R^2 >.79, therefore the selected models included BurstPressure and Gap as additive terms. The best models as determined by lowest AIC and highest adjusted R^2 are summarized in Tables 45 and 46. The predictive equations based on these models are given in Table 47.

Interpretation of results

No general predictive equations could be developed based on the adhesive-package and package-group models due to the variability in the parameter coefficients. However, the analysis performed over all packages provided models with fairly high R^2 values. Given the varied characteristics of the packages in the study, the equations developed based on these models may be generally applicable.

The Gap term has the highest regression coefficient, which indicates that the peel force responses are most sensitive to changes in gap distance.

Table 43. Best models for predicting peak and average force at burst location from burst pressure and gap by package group

Dependent Variable	Package Group	Model	Model ID	Intercept	Burst Pressure	Gap	Adjusted R^2	Prediction R^2	N	AIC	MSE	AIC rank	Selected by
PeakForce_at_BurstLoc	PS1 PS2 PS4 PS7	M21	M21-4	.	0.21	7.46	0.88	0.88	40	56.86	3.95	4	A and R
	PS3 PS6	M21	M21-1	.	0.52	2.03	0.95	0.94	30	7.08	1.19	1	A and R
AvgForce_at_BurstLoc	PS1 PS2 PS4 PS7	M22	M22-4	.	0.16	6.11	0.86	0.86	40	44.38	2.89	4	A and R
	PS3 PS6	M22	M22-1	.	0.45	1.42	0.93	0.93	30	4.41	1.09	1	A and R

Table 44. Best models for predicting lowest peak and lowest average force from burst pressure and gap by package group

Dependent Variable	Package Group	Model	Model ID	Intercept	Burst Pressure	Gap	Adjusted R^2	Prediction R^2	N	AIC	MSE	AIC rank	Selected by
LowPeakForce	PS1 PS2 PS4 PS7	M23	M23-4	.	0.19	5.95	0.88	0.88	40	39.11	2.53	4	A and R
	PS3 PS6	M23	M23-2	.	0.46	2.12	0.94	0.94	30	5.76	1.14	2	R
LowAvgForce	PS1 PS2 PS4 PS7	M24	M24-4	.	0.16	3.99	0.88	0.88	40	15.80	1.41	4	A and R
	PS3 PS6	M24	M24-2	.	0.41	1.45	0.93	0.93	30	-0.26	0.93	2	R

Table 45. Best models for predicting peak and average force at burst location from burst pressure and gap over all packages

Dependent Variable	Model	Model ID	Intercept	Burst Pressure	Gap	Adjusted R^2	Prediction R^2	N	AIC	MSE	AIC rank	Selected by
PeakForce_at_BurstLoc	M13	M13-4	.	0.32	5.26	0.83	0.83	124	187.05	4.45	4	R
AvgForce_at_BurstLoc	M14	M14-4	.	0.27	3.83	0.83	0.83	124	124.08	2.68	4	R

Table 46. Best models for predicting lowest peak and lowest average force from burst pressure and gap over all packages

Dependent Variable	Model	Model ID	Intercept	Burst Pressure	Gap	Adjusted R^2	Prediction R^2	N	AIC	MSE	AIC rank	Selected by
LowPeakForce	M15	M15-3	.	0.30	4.12	0.86	0.86	124	121.78	2.63	3	R
LowAvgForce	M16	M16-3	.	0.25	2.95	0.85	0.84	124	66.73	1.69	3	R

Table 47. Predictive equations for peel force based on burst pressure and gap

Equation	Adjusted R^2	Prediction R^2
Peak Force at Burst Location = 0.32*Burst Pressure + 5.26*Gap	.83	.83
Average Force at Burst Location = 0.27*Burst Pressure + 3.83*Gap	.83	.83
Lowest Peak Force = 0.30*Burst Pressure + 4.12*Gap	.86	.86
Lowest Average Force = 0.25*Burst Pressure + 2.95*Gap	.85	.84

CHAPTER IX

CONCLUSION

Summary and conclusions

A structured methodology, incorporating systematic sample preparation and matching, model generation through multiple linear regression, model scoring using Akaike's Information Criterion, and model cross-validation using PRESS statistics, was developed and used to compare medical device tray peel force and burst pressure and to develop empirical models explaining the relationships among burst pressure, peel force and the factors affecting them. Specifically, three families of models were developed. The first family of models predicts lowest peak and lowest average peel forces based on seal process parameters. The second model family predicts burst pressure based on seal process parameters, package characteristics, and restraining plate gap distance. The third family of models predicts peel force based on burst pressure and gap distance.

The research approach addressed six aspects of the modeling process that can affect the predictive ability of the resulting model. These are input data quality, sample representativeness, identification of candidate models, model selection criteria, model validation, and assessment of predictive ability.

To improve the quality of the input data, a structured methodology for sample identification and matching was used, and burst testing was standardized to a restrained burst test. To improve the representativeness of the sample upon which the models were based, trends in tray and lid materials were researched, and the materials expected to be most prevalent over the next five years were used. In addition, factorial designs were used to cover a wide range of process settings and to allow assessment of interactions. To generate candidate model forms, all possible subsets of several factors known or suspected to affect seal strength were generated. Selection of the best model from candidate models was accomplished using Akaike's Information Criterion (AIC) as the primary selection criterion and adjusted R^2 as the secondary criterion. Selected models were validated using the PRESS statistic for cross-validation, and the predictive ability of the models was assessed by calculating prediction R^2 values.

This research used alternative model evaluation criteria, rather than the traditionally used R^2 value. AIC was used as the primary selection criterion, to select from all possible subsets the smallest models with the best fit to the data. Adjusted R^2 statistics were used as a secondary selection criterion within the models preferred by AIC. Whereas the regular R^2 statistic increases with each term added to the model, regardless of whether the additional variable is statistically significant or not, AIC and adjusted R^2 apply a penalty for the addition of unnecessary variables, resulting in a higher assurance that the best model has been found.

PRESS statistics were calculated as a form of cross-validation of the models. All of the models have low PRESS values and high predictive R^2 values, so they may be expected to perform well in use. However, they will need to be validated on a wide scale in actual medical device packaging operations. With validation, the equations may be employed to allow the use of the burst test in ongoing process control activities, rather than the more laborious peel test.

Using the structured sample preparation and matching methodology, multiple locations around the tray perimeter were uniformly identified, tested, and compared. This methodology allowed the burst pressure at a specific tray location to be matched with the peel force at the same location—and other locations—on an identical tray, and agreement between burst location and minimum peel force locations to be evaluated. It was observed that burst location matched the lowest average force location at a higher percentage than it matched the lowest peak force location. For some packages the match percentages at the average force location were as high as 67%. The overall percent of agreement was 34% for lowest average force and 27% for lowest peak force. Calculation of match percentages within gap levels resulted in higher percentages for all packages, with 60% of packages having match percentages of 67% to 100%.

Over all packages, average peel force was lower than peak peel force. This finding and the observation of higher agreement between lowest average peel force location and burst location make a case for using average peel force as the preferred measure of minimum tensile seal strength. In addition, average peel force is preferred over peak peel force because it provides an unbiased estimate of the seal strength of the specimen and satisfies the requirement to verify that the seal strength of the package meets

the predetermined minimum seal strength specification. Peak force is by definition a maximum value, so it cannot represent the minimum seal strength.

Peel force values at multiple locations around the tray perimeter were evaluated and found to be non-uniform. Therefore, the selection of location for peel test specimens has a significant effect on the conclusions reached regarding the minimum seal strength of a package. Lower peel force values were seen near the corners of the tray, rather than in the centers of the sides. Similar results were observed in the burst pressure responses. Most packages tended to burst at or near a corner of the tray. Package designers and testers should consider this when specifying minimum peel strength requirements and when testing to verify achievement of the specification.

Two models to predict peak peel force and average peel force based on sealing process parameters were developed and showed good fit and predictive ability, with prediction R^2 values of .94 and .92, respectively. The equations from these models are repeated below.

$$\text{Peak Force} = 0.02*\text{Seal Temperature} - 0.02*\text{Seal Pressure} + 0.47*\text{DwellTime} \quad (9.1)$$

$$\text{Average Force} = 0.01*\text{Seal Temperature} - 0.02*\text{Seal Pressure} + 0.45*\text{DwellTime} \quad (9.2)$$

One model to predict burst pressure based on sealing, package, and burst test parameters was developed and showed good fit and predictive ability. The model has an expected predictive capability of .94. The equation from this model is repeated below.

$$\begin{aligned}\text{Burst Pressure} = {} & 0.01*\text{Seal Temperature} + 0.01*\text{Seal Pressure} \\ & + 0.11*\text{Dwell Time} - 1.12*\text{Gap} + 0.06*\text{Tray Volume} - 0.03*\text{Length-Width Ratio} \\ & - 1.21*\text{Tray Height} - 0.03*\text{Tray Area}\end{aligned} \quad (9.3)$$

Four models were developed for the prediction of four peel force responses from burst pressure and restraining plate gap distance. The models have expected predictive capabilities of .83 to .86. The equations from these models are repeated below.

$$\text{Peak Force at Burst Location} = 0.32*\text{Burst Pressure} + 5.26*\text{Gap} \quad (9.4)$$

$$\text{Average Force at Burst Location} = 0.27*\text{Burst Pressure} + 3.83*\text{Gap} \quad (9.5)$$

$$\text{Lowest Peak Force} = 0.30*\text{Burst Pressure} + 4.12*\text{Gap} \quad (9.6)$$

$$\text{Lowest Average Force} = 0.25*\text{Burst Pressure} + 2.95*\text{Gap} \quad (9.7)$$

Based on the high prediction R^2 values, the developed models can be expected to explain a high percentage of the variability in seal strength for new packages. However, the comparability of the results for diverse packaging operations or for a particular packaging operation over time will depend on the calibration state and maintenance level of the sealing equipment. It is important that the equipment be maintained in such way as to provide uniform temperature, pressure, and dwell time inputs to the tray sealing surface. These inputs need to be calibrated to NIST-traceable standards. In addition, the gaskets around the tray cavities must be maintained free of defects and replaced when worn, and all other equipment maintenance must be completed as required.

This research has met a need in the field of medical device packaging science for mathematical equations of seal strength, structured testing methodologies, and seal strength reference data. The use of the developed methodologies and models may increase the quantity and quality of tray testing performed in industry, enable manufacturers to develop more robust sealing processes, and ultimately reduce the number of package failures and recalls. The work that has been done has provided useful information, insight, and tools for medical device tray testing and has laid a foundation for future research in this area.

Suggestions for future research

There are several research efforts that can make use of the results of this research or build on the work done here.

The most important follow-on effort is to validate the predictive equations by applying them to diverse packaging processes and assessing how well the predictions agree with observed seal strengths. The structured methodology must be followed in order to have a valid comparison of the results.

Another important research effort would be to evaluate the equations using post-sterilization packages, determine if there is a decrease in seal strength after sterilization, and determine the factors to be applied to adjust for any observed decrease. The ultimate goal of seal strength testing is to ensure that packages remain sealed until the point of use by the user. To provide the most value, any predictive equations that are applied should be able to predict post sterilization seal strength.

Additionally, the research can be repeated using packages that are filled with product. The current research used empty trays. The addition of product to the trays may have an impact on the observed burst pressure, resulting in different coefficients for the models.

This research used adhesives from the family of water-based flood-coated adhesives. Further research could apply the same methodology using a wax-based hot-melt dot matrix adhesive to produce equations applicable to that type of adhesive.

Another useful extension of the research would be to evaluate the effect of seal width and incorporate it into the equations.

REFERENCES

1. Franks S. Medical package testing: It's come a long way, baby. originally published *Medical Device & Diagnostic Industry* 2004; **8:** 162 et seq.; http://www.devicelink.com/mddi/archive/04/08/025.html [accessed 19 January 2005].

2. Franks S, Barcan D. Comparing tensile and inflation seal-strength tests for medical pouches. originally published *Medical Device & Diagnostic Industry* 1999; **8:** 60 et seq.; http://www.devicelink.com/mddi/archive/99/08/006.html [accessed 11 August 2004].

3. Franks S. Strength and integrity: the basics of medical package testing. *Technical Paper*. T.M. Electronics: Boylston, MA, 2001.

4. Franks S. Strength and integrity, part two: Basics of seal-strength testing. *Pharmaceutical & Medical Packaging News* 2002; **6:** 52-53.

5. Feliú-Báez R, Lockhart H, Burgess G. Correlating peel and burst tests for sterile medical device packages. originally published *Medical Device & Diagnostic Industry* 2003; **January**; http://www.devicelink.com/mddi/archive/03/01/002.html [accessed 11 August 2004].

6. Feliú-Báez R, Lockhart H. Effect of plate separation on restrained burst test. *Packaging Technology and Science* 2003; **16:** 191-198.

7. Feliú-Báez R, Lockhart H, Burgess G. Correlation of peel and burst tests for pouches. *Packaging Technology and Science* 2001; **14**: 63-69.

8. ASTM. *Standard Test Method for Determining Integrity of Seals for Medical Packaging by Visual Inspection, ASTM F 1886-98*. American Society for Testing and Materials: West Conshohocken, PA, 2004.

9. ASTM. *Standard Test Method for Seal Strength of Flexible Barrier Materials, ASTM F 88-07*. American Society for Testing and Materials: West Conshohocken, PA, 2007.

10. ASTM. *Standard Test Method for Burst Testing of Flexible Package Seals Using Internal Air Pressurization Within Restraining Plates, ASTM F 2054-00*. American Society for Testing and Materials: West Conshohocken, PA, 2000.

Supplemental Sources Consulted

AAMI. *Packaging for Terminally Sterilized Medical Devices, ANSI/AAMI/ISO 11607:2006*. Association for the Advancement of Medical Instrumentation: Arlington, VA, 2006.

ASTM. *Standard Test Methods for Internal Pressurization Failure Resistance of Unrestrained Packages for Medical Applications, ASTM F 1140-00*. American Society for Testing and Materials: West Conshohocken, PA, 2000.

Barcan D. Exposing the myths of tensile seal strength testing. *Pharmaceutical & Medical Packaging News* 2004; **4**: 26-28.

FDA. *Quality System Regulation, 21 CFR Part 820*. U.S. Food and Drug Administration: Washington D.C., 1996.

Franks S. Flexible Package Seal Strength Testing. *Technical Paper*. T.M. Electronics: Boylston, MA, 1996; http://www.tmelectronics.com/Pages/iopp.html [accessed 18 December 2002].

Franks S. Calculating factors of safety for package burst and creep test fixtures. *Medical Device & Diagnostic Industry* 1998; **1**: 157-163.

Franks M, Franks S. Testing Medical Device and Package Integrity. *Technical Paper*. T.M. Electronics: Boylston, MA, 1999; http://www.tmelectronics.com/Pages/mfpaper.html [accessed 18 December 2002].

Franks S. Strength and integrity: the basics of medical package testing. *Pharmaceutical & Medical Packaging News* 2002; **1**: 28-33.

Garcia-Diaz A, Phillips DT. *Principles of Experimental Design and Analysis*. Chapman & Hall: London, 1995.

Montgomery D. *Design and Analysis of Experiments*. Wiley: New York, 2001.

Swain E. Putting standards to the test. *Pharmaceutical & Medical Packaging News* 2000; **January:** 38 et seq.; http://www.devicelink.com/pmpn/archive/00/01/005.html [accessed 18 November 2004].

APPENDIX A

LIST OF SEPARATE APPENDIX FILES

Separate Appendix files accompany this dissertation and are available for downloading.

FILE	DESCRIPTION
Appendix A1.pdf	TRAY DIAGRAMS FOR PACKAGES PS1-PS9
Appendix A2.pdf	PEAK PEEL FORCE SPECIMEN DESCRIPTIVE STATISTICS
Appendix A3.pdf	PEEL TEST FORCE PROFILES, GROUPED BY ADHESIVE, PACKAGE AND SPECIMEN LOCATION
Appendix A4.pdf	PEEL TEST FORCE PROFILES, GROUPED BY ADHESIVE, POINT NUMBER AND SPECIMEN CATEGORY
Appendix A5.pdf	BOX PLOTS OF PEEL FORCE FOR PACKAGE, BYADHESIVE, POINT NUMBER AND SPECIMEN CATEGORY
Appendix A6.pdf	PLOTS OF PEAK FORCE FOR SPECIMENS WITHIN EACH TRAY SAMPLE, GROUPED BY PACKAGE
Appendix A7.pdf	PLOTS OF PEAK FORCE FOR SPECIMENS WITHIN EACH TRAY SAMPLE, GROUPED BY POINT NUMBER
Appendix A8.pdf	BOX PLOTS OF PEEL FORCES FOR PACKAGE AND SPECIMEN LOCATION, BY ADHESIVE AND POINT NUMBER
Appendix A9.pdf	HISTOGRAM OF LOWEST PEAK FORCE LOCATION ACROSS ALL SPECIMENS
Appendix A10.pdf	HISTOGRAMS OF LOWEST PEAK FORCE LOCATION BY PACKAGE AND ADHESIVE
Appendix A11.pdf	HISTOGRAMS OF LOWEST PEAK FORCE LOCATION BY POINT NUMBER AND ADHESIVE
Appendix A12.pdf	MODEL SUMMARY FOR REGRESSION OF PEEL FORCE ON SEALING PARAMETERS BY ADHESIVE AND PACKAGE
Appendix A13.pdf	MODEL SUMMARY FOR REGRESSION OF PEEL FORCE ON SEALING PARAMETERS BY PACKAGE GROUP
Appendix A14.pdf	MODEL SUMMARY FOR REGRESSION OF PEEL FORCE ON SEALING PARAMETERS – OVERALL
Appendix A15.pdf	AVERAGE PEEL FORCE SPECIMEN DESCRIPTIVE STATISTICS

FILE	DESCRIPTION
Appendix A16.pdf	PLOTS OF AVERAGE FORCE FOR SPECIMENS WITHIN EACH TRAY SAMPLE, GROUPED BY PACKAGE
Appendix A17.pdf	PLOTS OF AVERAGE FORCE FOR SPECIMENS WITHIN EACH TRAY SAMPLE, GROUPED BY POINT NUMBER
Appendix A18.pdf	HISTOGRAM OF LOWEST AVERAGE FORCE LOCATION ACROSS ALL SPECIMENS
Appendix A19.pdf	HISTOGRAMS OF LOWEST AVERAGE FORCE LOCATION BY PACKAGE AND ADHESIVE
Appendix A20.pdf	HISTOGRAMS OF LOWEST AVERAGE FORCE LOCATION BY POINT NUMBER AND ADHESIVE
Appendix A21.pdf	PLOTS OF PEEL FORCE AND BURST PRESSURE RESPONSES VS PARAMETER LEVELS
Appendix A22.pdf	BURST PRESSURE SAMPLE DESCRIPTIVE STATISTICS
Appendix A23.pdf	HISTOGRAM OF BURST LOCATION ACROSS ALL PACKAGES
Appendix A24.pdf	HISTOGRAMS OF BURST LOCATION BY PACKAGE AND ADHESIVE
Appendix A25.pdf	HISTOGRAMS OF BURST LOCATION BY SEAL SETTING AND ADHESIVE
Appendix A26.pdf	HISTOGRAM OF BURST LOCATION BY SEAL SETTING, GAP AND ADHESIVE
Appendix A27.pdf	MODEL SUMMARY FOR REGRESSION OF BURST PRESSURE ON SEALING, PACKAGE, AND BURST TEST PARAMETERS BY ADHESIVE AND PACKAGE
Appendix A28.pdf	MODEL SUMMARY FOR REGRESSION OF BURST PRESSURE ON SEALING, PACKAGE, AND BURST TEST PARAMETERS BY PACKAGE GROUP
Appendix A29.pdf	MODEL SUMMARY FOR REGRESSION OF BURST PRESSURE ON SEALING, PACKAGE, AND BURST TEST PARAMETERS - OVERALL
Appendix A30.pdf	BURST PRESSURE AND PEEL FORCE COMBINED DATA
Appendix A31.pdf	MODEL SUMMARY FOR REGRESSION OF PEEL FORCE ON BURST PRESSURE BY ADHESIVE AND PACKAGE
Appendix A32.pdf	MODEL SUMMARY FOR REGRESSION OF PEEL FORCE ON BURST PRESSURE BY PACKAGE GROUP
Appendix A33.pdf	MODEL SUMMARY FOR REGRESSION OF PEEL FORCE ON BURST PRESSURE – OVERALL
Appendix A34.pdf	PLOTS OF SEAL STRENGTH RESPONSES VS PARAMETER LEVELS

FILE	DESCRIPTION
Appendix A35.pdf	GRAPHICAL ANALYSIS OF ADHESIVE EFFECT ON PEEL FORCE
Appendix A36.pdf	GRAPHICAL ANALYSIS OF ADHESIVE EFFECT ON BURST PRESSURE

VITA

Name: Patricia Mays

Address: Texas A&M, Department of Industrial and Systems Engineering, 3131 TAMU, College Station, TX 77845

Email Address: pfmays08@yahoo.com

Education:
Ph.D., Industrial Engineering, Texas A&M University, 2008
M.S., Industrial Engineering, University of Arkansas at Fayetteville, 1995
B.S., Industrial Engineering, University of Arkansas at Fayetteville, 1986

Certifications:
Certified Quality Manager, American Society for Quality, 2005
Certified Quality Auditor, American Society for Quality, 2005
Certified Lead Auditor, ISO 9001:2000, Det Norske Veritas, 2001

Licenses:
Licensed Professional Engineer, Arkansas, Industrial Engineering, 1993
Licensed Christian Minister, 2003

Memberships:
American Society for Quality, Senior Member
Institute of Industrial Engineers, Senior Member
National Society of Professional Engineers
National Association of Female Executives
Alpha Kappa Alpha Sorority

Professional Experience:

EnQual Solutions 2004-Present
Owner and Principal Consultant helping organizations find solutions to systems engineering and quality problems
www.enqual.net, mail@enqual.net

Boston Scientific Corporation 2006-2008
Principal Quality Engineer, Design Assurance

Tecan Systems, Inc. 2005-2006
Director of Quality Assurance and Regulatory Affairs

NeuroPace, Inc 2001-2004
Senior Quality Engineer

Applied Materials, Inc. 1999-2001
Reliability Specialist/Quality Engineer

General Dynamics Electronics 1987-1992
Industrial/Manufacturing Engineer